

Characterization of DNA methylation clock algorithms applied to diverse tissue types

Mark Richardson¹, Courtney Brandt¹, Niyati Jain¹, James L. Li¹, Kathryn Demanelis², Farzana Jasmine¹ Muhammad G. Kibriya¹, Lin Tong¹, Brandon L. Pierce^{1,3,4}

¹Department of Public Health Sciences, University of Chicago, Chicago, IL 60615, USA

²Department of Medicine, University of Pittsburgh, Pittsburgh, PA 15261, USA

³Department of Human Genetics, University of Chicago, Chicago, IL 60615, USA

⁴Comprehensive Cancer Center, University of Chicago, Chicago, IL 60615, USA

Correspondence to: Brandon L. Pierce; **email:** brandonpierce@uchicago.edu

Keywords: epigenetic aging, epigenetic clock, DNA methylation

Received: December 5, 2023

Accepted: December 12, 2024

Published: January 3, 2025

Copyright: © 2025 Richardson et al. This is an open access article distributed under the terms of the [Creative Commons Attribution License](https://creativecommons.org/licenses/by/4.0/) (CC BY 4.0), which permits unrestricted use, distribution, and reproduction in any medium, provided the original author and source are credited.

ABSTRACT

Background: DNA methylation (DNAm) data from human samples has been leveraged to develop “epigenetic clock” algorithms that predict age and other aging-related phenotypes. Some DNAm clocks were trained using DNAm obtained from blood cells, while other clocks were trained using data from diverse tissue/cell types. To assess how DNAm clocks perform across non-blood tissue types, we applied DNAm algorithms to DNAm data generated from 9 different human tissue types.

Methods: We generated array-based DNAm measurements for 973 samples from deceased tissue donors from the GTEx (Genotype Tissue Expression) project representing nine distinct tissue types: lung, colon, prostate, ovary, breast, kidney, testis, skeletal muscle, and whole blood. For all samples, we generated DNAm clock estimates for 8 epigenetic clocks and characterized these tissue-specific clock estimates in terms of their distributions, correlations with chronological age, correlations of clock estimates between tissue types, and association with participant characteristics.

Results: For each clock, the mean DNAm age estimate varied substantially across tissue types, and the mean values for the different clocks varied substantially within tissue types. For most clocks, the correlation with chronological age varied across tissue types, with blood often showing the strongest correlation. Each clock showed strong correlation across tissues, with some evidence of some residual correlation after adjusting for chronological age. In lung tissue, smoking generally had a positive association with epigenetic age.

Conclusions: This work demonstrates how differences in epigenetic aging among tissue types leads to clear differences in DNAm clock characteristics across tissue types. Tissue or cell-type specific epigenetic clocks are needed to optimize predictive performance of DNAm clocks in non-blood tissues and cell types.

INTRODUCTION

Changes in the human epigenome occur as humans age, and these epigenetic alternations are considered a hallmark (and a cause) of human aging [1]. One such epigenetic feature is DNA methylation (DNAm) at cytosine-guanine dinucleotides. DNAm plays a key role

in gene regulation, particularly DNAm at CpG islands near gene promoters, which is indicative of gene silencing [2]. Early studies of aging and DNAm reported age-related changes in cancer cells [3, 4], human tissues [5], mouse tissues [6], as well as in blood samples from twin studies [7]. Subsequent studies identified regions enriched for aging-related DNAm

changes, including promoters of Polycomb group protein target genes [8] and bivalent chromatin domains [9]. Associations between age and DNAm at CpG sites across the human genome have been thoroughly characterized in many studies (most often based on DNAm data from blood cells) [2, 10, 11], and these age-related changes are likely accompanied by changes in other epigenetic features (e.g., histone modifications, nucleosome positioning, chromatin conformation) [8, 12]. While our understanding of these changes and their implications for cellular function is incomplete, the concepts of “loss of constitutive heterochromatin” and “epigenetic drift” have been used to describe how these changes relate to aging [12].

In human studies, DNAm data has often been generated using commercial arrays that measure DNAm at ~27,000 to ~850,000 CpG sites. These data have been used to develop DNA methylation (DNAm) clock algorithms that leverage data on many CpG sites to predict age and other aging-related phenotypes [2, 11, 13]. First generation DNAm clocks (i.e., Hannum clock and Horvath clock) were trained with the goal of accurately estimating chronological age of a biological sample. These clocks estimate acceleration of biological age (relative to chronological age), a measurement that has been shown to positively correlate with aging-related phenotypes [2]. Later generations of DNAm clocks (e.g., GrimAge [14], PhenoAge [15]) were trained on additional health- and aging-related variables (e.g., smoking, circulating biomarkers) in order to generate biological aging estimates that more strongly predict health and lifespan. Additional DNAm clocks of interest include “mitotic clocks”, such as EpiTOC (Epigenetic Timer of Cancer), which estimates the mitotic age of cells, how many stem cell divisions have occurred, and provides a subsequent estimate of cell age [16]. In recent years, clocks have been developed that use larger numbers of CpGs, and sophisticated variable selection methods, in order to improve prediction of chronological age, including Vijayakumar and Cho’s “EpiClock” (~7000 CpGs) [17], AltumAge (20,318 CpGs) [18], and the Zhang clock (514 CpGs) [19]. In addition, a clock that estimates “pace of aging” (DunedinPACE) was developed using two decades of longitudinal biomarker data (173 CpGs) [20].

The DNAm clocks developed to date were trained using either (1) DNAm obtained from blood cells only, or (2) DNAm obtained from diverse tissue types, but with the majority of training data coming from blood cells [11]. Thus, DNAm clocks may not perform equally well across tissue types, and few studies have compared the performance of DNAm aging clock algorithms across a variety of non-blood tissue types [21, 22]. It is important to understand clocks’ performance across

different tissues, as clinical applications may rely on accessible tissues only to assess tissue-specific aging; and forensic settings may rely on accurate age prediction from a variety of tissue sources.

To assess differences across tissues with respect to biological age predictions, we used DNAm data from the Genotype-Tissue Expression (GTEx) Project to obtain epigenetic age estimates for DNAm clocks (Horvath, Hannum, PhenoAge, EpiTOC, EpiClock, AltumAge, Zhang, and Dunedin PACE) across 9 different tissue types (lung, colon, prostate, ovary, breast, kidney, testis, skeletal muscle, and whole blood). We characterize DNAm aging estimates across tissues in terms of the (1) distribution of DNAm clock estimates, (2) strength of each clock’s association with age, (3) correlation of clock estimates between tissue types, and (4) associations of participant characteristics with clock estimates.

MATERIALS AND METHODS

Tissue samples

The GTEx Project is a publicly available biobank of >17,000 human tissue samples collected from ~950 post-mortem multi-tissue donors, with ~50 unique human tissue types represented [23]. The GTEx project has generated genome-wide data on genetic variation (using whole-genome sequencing) and gene expression (using RNA sequencing) for >15,000 tissue samples from >800 donors [24]. For each donor, characteristics such as age, race, BMI, and sex are also publicly available [25].

The “enhancing GTEx” (eGTEx) initiative built upon the core GTEx data by adding complementary layers of biological information, including proteomics, DNA and RNA modifications, and telomere length (TL) [26]. As a part of eGTEx, we generated array-based DNAm measurements for ~1,000 GTEx samples, described previously [27]. The selection of tissue types was based on several considerations, including inclusion of cancer-relevant tissues (lung, colon, prostate, ovary, breast, kidney), tissues with unique aging biology (testis, skeletal muscle), and tissues commonly used in epidemiological research (whole blood).

Genome-wide DNA methylation measurement and processing

We measured DNAm at 866,895 CpG sites throughout the epigenome in 1,000 GTEx tissue samples from 9 unique tissue types obtained from 424 GTEx subjects using the Infinium MethylationEPIC v1 array (Illumina,

San Diego, CA, USA). DNA samples were extracted from GTEx tissue samples using Qiagen Genra Puregene method at GTEx Laboratory Data, Analysis and Coordinating Center (LDACC), and sent to the Institute for Population and Precision Health Laboratory at the University of Chicago on 96-well plates. Neither tissue types nor individuals were not batched by plate. Bisulfite conversion was applied to 500 ng of DNA using EZ-96 DNA methylation kit (Zymo Research, Irvine, CA, USA). All samples were then prepared and analyzed in accordance with the manufacturer guidelines and protocol for the EPIC array.

DNAm data was processed with ChAMP software [28]. Raw DNAm values were background-adjusted using the single sample normal-exponential out-of-band (*ssnoob*) method with dye bias correction [29, 30]. DNAm beta values were normalized using the beta mixture quantile (BMIQ) method, adjusting for type I/II probe bias [31]. After normalization, we removed one additional sample with array-derived genotype profile not matching WGS-derived one. As described previously [27], principal component analysis (PCA) was conducted on DNAm beta values within each tissue type, and 3 samples were removed for being outliers with respect to the top 5 principal components (PCs) of the corresponding tissue. We additionally removed 13 breast samples obtained from males (leaving only female breast samples for analysis), resulting in 973 samples for analyses purposes (representing 9 tissue types and 424 donors). Due to missing telomere and smoking status data, an additional 99 samples were removed (from the regression analyses only) resulting in 874 samples.

DNAm clock estimates

For this study, we selected several commonly-used clocks, as well as recently developed clocks, including both pan-tissue and blood-specific clocks (Table 1). We excluded clocks that use chronological age as input (i.e., GrimAge). We acknowledge there are additional clocks described in the literature that we are not assessing in this work. DNAm clock estimates for all 973 GTEx tissues samples were obtained using the Horvath group's online epigenetic clock calculator [32] and the R code provided [33]. Three of the DNAm clocks we analyzed were provided by the calculator: Horvath, Hannum, PhenoAge. Clock estimates for EpiTOC [16], EpiClock [17], AltumAge [34], Zhang clock [19], and DundinPACE [20] were obtained using code provided by the authors. For each of the clock algorithms examined, we provide information on the training data, arrays and CpGs used, the clock's intended purpose and the number of clock CpGs that were missing from our dataset (i.e., removed during QC) (Table 1).

The Horvath clock [33] and Hannum clock [35], considered first-generation clocks, were trained with the goal of accurately estimating chronological age based on DNAm values measured from samples. PhenoAge is considered a second-generation clock that reflects both lifespan and health and was trained on age and 9 blood biomarkers [15]. Because the GrimAge clock [14] uses age as an input, we did not evaluate GrimAge in this work, as age prediction is a primary focus of this paper.

EpiTOC (Epigenetic timer of cancer) [16] is a “mitotic” clock was developed to capture the amount of stem cell division in a tissue. EpiTOC uses 385 CpGs selected based on (1) location within promoters that localize Polycomb group target genes, (2) lack of methylation in a variety of fetal tissue types, and (3) increasing methylation with age in human blood samples.

The EpiClock algorithm was developed to predict chronological age across multiple tissue types [17]. The AltumAge algorithm, another multi-tissue clock, was trained using a neural network approach and is reported to have enhanced performance for older ages and for diverse tissue types.

The Zhang clock was developed from the stated goal of examining whether the association between the age acceleration residual of different predictors (developed by the researchers in the same paper) and death is affected by improving predictive power as its training set sample size increases and by correcting for confounders. The final CpG count was 514, chosen based on their associations with chronological age in blood samples.

DunedinPACE uses DNA methylation data from blood samples for 173 CpGs to determine the “Pace of Aging” of a person. This clock is based on biological changes observed for 19 indicators of organ-system integrity over two decades in the Dunedin birth cohort [20].

Among the CpGs in our post-QC dataset, we were missing a small percentage for the CpGs used by each clock (Table 1).

Estimation of immune cell infiltration

The presence of leukocytes in GTEx samples was estimated using the LUMP algorithm [36], which leverages data on 44 CpG sites that are specifically methylated specifically in immune cells. LUMP provides a percentage representing “purity”, so we subtracted this percentage from 1 to obtain a percentage represented immune cell infiltration (ICI). To determine if ICI impacts clock performance, we first examined the association between the average immune cell infiltration

Table 1. Summary of the clock algorithms examined in this work.

Clock	Tissue type(s) for training	Array(s) used	Purpose	Training data age	Ref	# CpGs used	# CpGs missing
Horvath	Multi-tissue (~8,000 samples)	27K and 450K	Estimate chronological age	Mean: 43 y Range: 0-100 y	33	353	23
Hannum	Whole blood (656 samples)	450K	Estimate chronological age	Mean: ~65 y Range: 19-101y	35	71	9
Pheno Age	Whole blood (9,926 samples)	27K, 450K, and 850K	Health + lifespan estimation	Mean age: 49y Range: 8-80y (NHANES)	15	513	12
Altum Age	Multi-tissue	27K, 450K, and 850K	Estimate chronological age	Mean: ~50 y Range: 0 to >100 y	18	20,318	522
EpiTOC	Fetal tissues and blood	450K	Capture stem cell divisions	Mean: ~65 y Range: 19-101y	16	385	31
EpiClock	Multi-tissue (3,114 samples)	450K, and 850K	Estimate chronological age	Median: 36.5 y Range: 0-103 y	17	6,761	515
Dunedin PACE	Whole blood (1,037 samples)	805K	Estimate pace of aging	Longitudinal birth cohort (sampled at 26, 32, 38, 45 y)	20	173	0
Zhang	Blood/saliva (13,661 samples)	450K and 850K	Estimate chronological age	Mean: 15-82 y (14 cohorts) Range: 2-104 y	19	514	8

(for a specific tissue) and the correlation between chronological age and clock age (for a specific tissue), across all eight non-blood tissue types. We also examined the interaction between chronological age and ICI (in relation to clock age) for each clock, in each tissue type.

Statistical analyses

We examined the distributions of all five biological clock estimates (across tissue types) using histograms, ridge plots, and violin plots. Acceleration for each clock was calculated as the residuals from a linear regression of the clock estimates on chronological age. To examine the strength of associations of clock estimates with participant characteristics (and age), we used linear regression and/or Pearson's correlation analysis. We calculated (1) the mean deviation for each clock applied to each tissue (i.e., average difference between clock age and chronological age) as well as (2) the median absolute error (i.e., median absolute difference between DNAm age and chronological age), similar to previous work [33]. We also used Pearson's correlation and linear regression to examine the association between clock estimates obtained from different tissue types. Linear regression models included sex, smoking, BMI, and telomere length as covariates. Telomere length was measured for GTEx samples as previously described [37].

RESULTS

The characteristics of the GTEx donors for each tissue type used for this project are described in Table 2. The

sample sizes for each tissue type ranged from 38 (female breast) to 212 (lung), with a total of 424 donors contributing tissue samples.

The tissue-specific distributions of chronological age and estimated DNAm ages (for each clock examined) are shown in Figure 1. The mean chronological age for donors varied somewhat across tissue types (~50 to ~62 years). For each clock examined, estimates varied substantially across tissue types, with mean clock estimates close to 0 years in some scenarios (i.e., PhenoAge for ovary) and close to 100 years other scenarios (i.e., AltumAge for kidney). For each clock, testis and ovary tissue tended to have lower (younger) clock estimates, while colon and lung tended to have higher (older) clock estimates compared to other tissue types.

The distribution of each clock within tissue type is shown in Figure 2. In whole blood, the distribution of each clock (considering both the mean and the variance), was most similar to chronological age, compared to other tissue types. The whole blood had low median absolute errors (Supplementary Table 1) and mean deviations (Supplementary Table 2) compared to other tissue types (for all clocks except AltumAge). The distributions of the Horvath (light brown) and EpiClock (blue) clocks most closely resembled the chronological age distributions (across most tissue types), with correspondingly small median absolute errors and mean deviations (Supplementary Tables 1, 2). The means of the blood-based clocks (PhenoAge and Hannum) tended to be lower than chronological age, with large negative mean deviations, in most tissue types (except in whole

Table 2. GTEx donor characteristics for each tissue type.

Total (n=973)	Breast (n=38)	Colon (n=224)	Kidney (n=50)	Lung (n=223)	Muscle (n=47)	Ovary (n=164)	Prostate (n=123)	Testis (n=50)	Whole Blood (n=54)
Age (years)									
Mean (SD)	50.0 (11.9)	56.1 (11.3)	59.7 (8.26)	55.2 (11.1)	57.1 (10.5)	50.6 (13.7)	54.1 (13.0)	54.2 (12.2)	50.3 (12.9)
Median [Min, Max]	50.5 [21, 70]	59.0 [21, 70]	61.5 [36, 70]	57.0 [22, 70]	60.0 [31, 70]	52.0 [21, 70]	57.0 [20, 70]	56.0 [22, 70]	52.5 [22, 70]
Sex									
Male	0 (0%)	156 (69.6%)	39 (78.0%)	160 (71.7%)	28 (59.6%)	0 (0%)	123 (100%)	50 (100%)	45 (83.3%)
Female	38 (100%)	68 (30.4%)	11 (22.0%)	63 (28.3%)	19 (40.4%)	164 (100%)	0 (0%)	0 (0%)	9 (16.7%)
Race									
Non-Hispanic White	0 (0%)	3 (1.3%)	0 (0%)	3 (1.3%)	0 (0%)	2 (1.2%)	0 (0%)	0 (0%)	0 (0%)
African American	6 (15.8%)	22 (9.8%)	6 (12.0%)	28 (12.6%)	6 (12.8%)	27 (16.5%)	10 (8.1%)	3 (6.0%)	5 (9.3%)
Other	32 (84.2%)	197 (87.9%)	44 (88.0%)	190 (85.2%)	41 (87.2%)	134 (81.7%)	111 (90.2%)	47 (94.0%)	48 (88.9%)
Missing	0 (0%)	2 (0.9%)	0 (0%)	2 (0.9%)	0 (0%)	1 (0.6%)	2 (1.6%)	0 (0%)	1 (1.9%)
BMI (kg/m2)									
Mean (SD)	25.4 (3.94)	27.1 (3.94)	26.4 (3.75)	27.6 (3.91)	26.8 (4.38)	26.8 (4.23)	27.1 (3.81)	27.2 (3.82)	27.4 (4.18)
Median [Min, Max]	25.5 [18.9, 33.3]	27.2 [18.8, 35.0]	26.6 [18.8, 34.8]	27.4 [18.6, 35.0]	26.6 [18.6, 34.4]	26.6 [18.5, 34.9]	27.1 [18.8, 34.9]	27.1 [19.0, 34.8]	27.2 [19.8, 35.0]
Smoker									
No	11 (28.9%)	57 (25.4%)	10 (20.0%)	62 (27.8%)	12 (25.5%)	57 (34.8%)	38 (30.9%)	12 (24.0%)	12 (22.2%)
Yes	27 (71.1%)	152 (67.9%)	37 (74.0%)	150 (67.3%)	34 (72.3%)	96 (58.5%)	73 (59.3%)	36 (72.0%)	40 (74.1%)
Missing	0 (0%)	15 (6.7%)	3 (6.0%)	11 (4.9%)	1 (2.1%)	11 (6.7%)	12 (9.8%)	2 (4.0%)	2 (3.7%)
Telomere length									
Mean (SD)	1.06 (0.314)	1.09 (0.386)	1.01 (0.339)	0.930 (0.228)	1.39 (0.352)	1.29 (0.291)	1.09 (0.294)	1.97 (0.522)	0.836 (0.206)
Median [Min, Max]	1.02 [0.37, 1.96]	1.07 [0.31, 2.59]	0.96 [0.32, 1.88]	0.91 [0.35, 1.72]	1.34 [0.89, 2.41]	1.25 [0.71, 2.24]	1.05 [0.19, 2.16]	1.93 [1.18, 3.45]	0.87 [0.37, 1.20]
Missing	1 (2.6%)	5 (2.2%)	0 (0%)	19 (8.5%)	4 (8.5%)	13 (7.9%)	0 (0%)	4 (8.0%)	1 (1.9%)

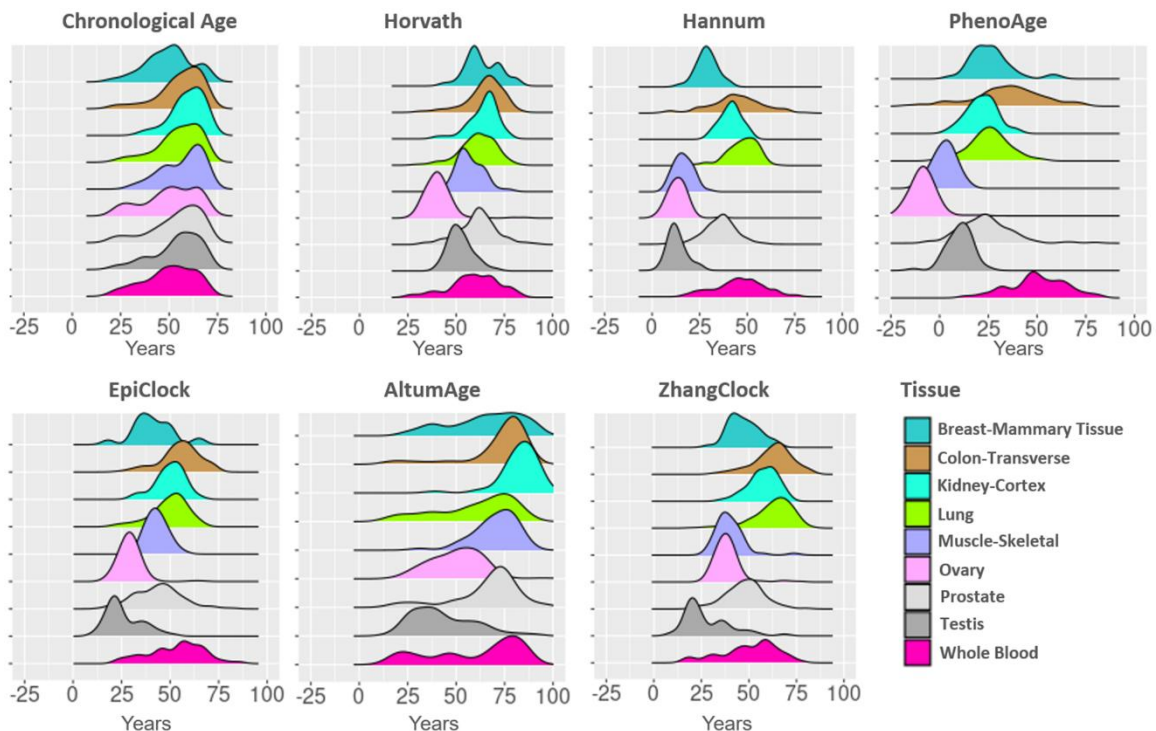


Figure 1. DNA methylation clock estimates vary across tissue types. The distributions of estimates for age and six clocks are color coded by tissue type. For each clock, tissue types are ranked by their median and color-coded. The median and inter-quartile ranges are shown as vertical lines.

blood), and high median absolute errors (Supplementary Tables 1, 2). In general, the clocks' distributions deviated most from chronological age in muscle, testis, and ovary tissues.

The correlation between each tissue-specific clock estimate and individuals' chronological age is shown in Table 3. For all clocks except EpiTOC, the clock estimates from blood showed the strongest correlation with chronological age, as compared to all other tissue types. For each clock, the correlation with chronological age varied substantially across tissue types. For most non-blood tissue types (including breast, colon, kidney, lung, ovary, prostate) the Hannum and PhenoAge clocks, both specifically designed for blood DNAm data, showed weaker correlation with chronological age than the clocks designed for pan-tissue applications (Horvath, AltumAge, and EpiClock). EpiTOC clock

was positively correlated with chronological age ($P < 0.05$) in all tissue types except for breast and muscle.

For each clock, we attempted to estimate the correlation in clock estimates between pairs of tissue types, using data from donors with DNAm data available for both tissue types. For each clock, there was clear correlation across tissue types (Supplementary Tables 3–9 and Supplementary Figures 1–6), with an average tissue-tissue correlation of 0.71 for Horvath, 0.47 for Hannum, 0.47 for PhenoAge, 0.15 for EpiTOC, 0.78 for AltumAge, 0.65 for EpiClock, and 0.65 for Zhang (based on 32 possible tissue-tissue pairs) (Figure 3A). Since lung and colon had the largest sample size (146 donors with DNAm data for both tissue types) and the most power/precision for assessing correlation between

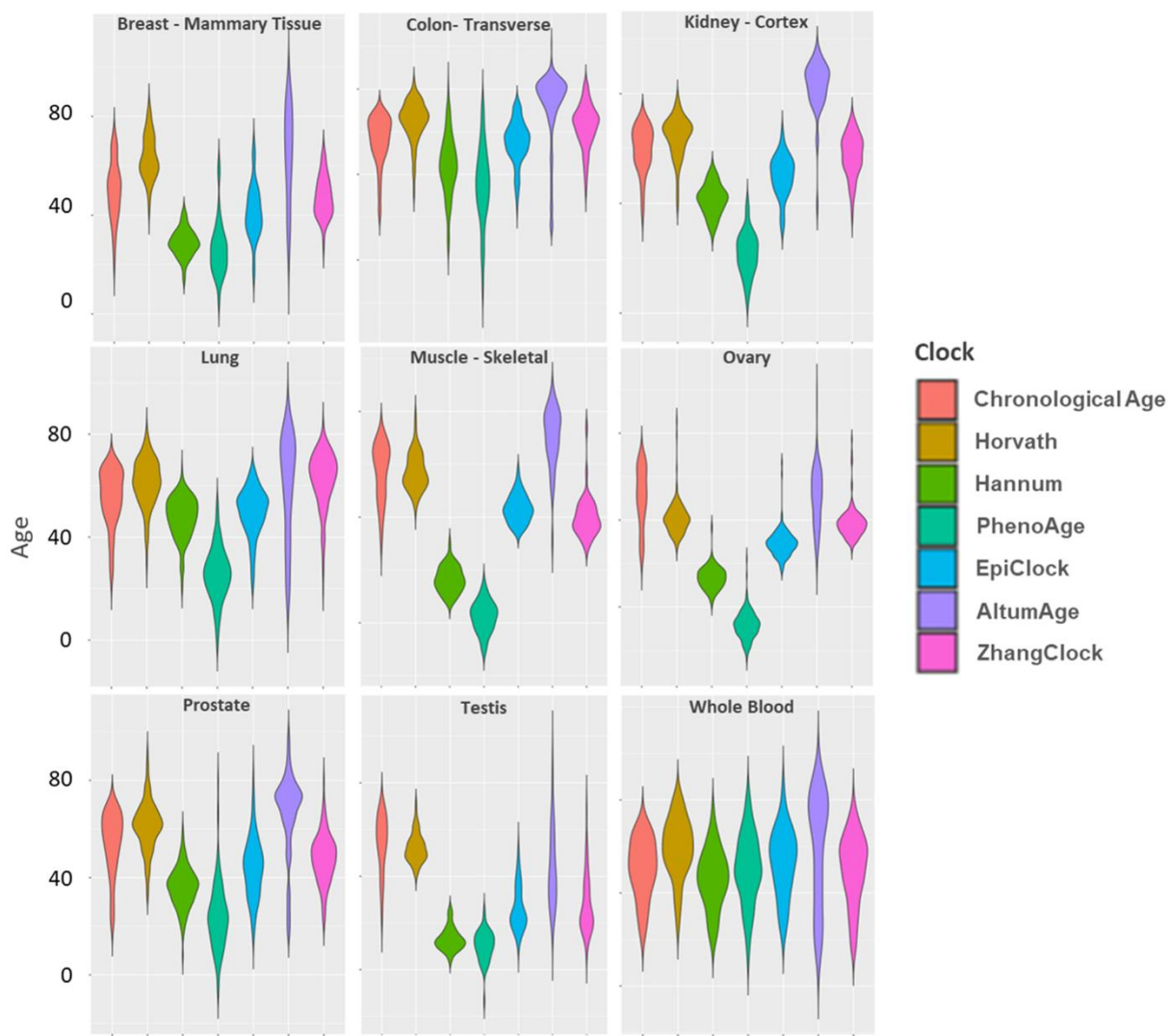


Figure 2. Distributions of chronological age and DNAm clock estimates within each of nine GTEx tissue types.

Table 3. Pearson correlations (and confidence intervals) between clock estimates and chronological age by tissue type.

Tissue	DNAm clocks						
	Horvath	Hannum	PhenoAge	EpiClock	AltumAge	EpiTOC	ZhangClock
Breast	0.78 (0.62-0.88)	0.73 (0.54-0.85)	0.57 (0.30-0.75)	0.86 (0.74-0.92)	0.85 (0.74-0.92)	0.10 (-0.23-0.41)	0.86 (0.74-0.92)
Colon	0.89 (0.86-0.91)	0.39 (0.27-0.50)	0.36 (0.25-0.47)	0.78 (0.72-0.83)	0.88 (0.85-0.91)	0.33 (0.20-0.44)	0.71 (0.63-0.77)
Kidney	0.89 (0.81-0.93)	0.82 (0.69-0.89)	0.67 (0.47-0.80)	0.90 (0.82-0.94)	0.84 (0.73-0.91)	0.49 (0.24-0.68)	0.91 (0.84-0.95)
Lung	0.87 (0.83-0.90)	0.85 (0.81-0.88)	0.71 (0.64-0.77)	0.92 (0.90-0.94)	0.93 (0.91-0.94)	0.36 (0.24-0.47)	0.84 (0.8-0.88)
Muscle	0.54 (0.30-0.72)	0.58 (0.35-0.74)	0.46 (0.19-0.66)	0.72 (0.54-0.83)	0.84 (0.72-0.91)	0.28 (-0.003-0.53)	0.46 (0.2-0.66)
Ovary	0.58 (0.47-0.67)	0.53 (0.41-0.63)	0.26 (0.12-0.40)	0.61 (0.50-0.70)	0.72 (0.64-0.79)	0.16 (0.01-0.31)	0.50 (0.37-0.61)
Prostate	0.86 (0.81-0.90)	0.60 (0.48-0.71)	0.67 (0.56-0.76)	0.81 (0.74-0.86)	0.91 (0.87-0.93)	0.38 (0.22-0.52)	0.71 (0.61-0.79)
Testis	0.69 (0.52-0.82)	0.65 (0.45-0.78)	0.77 (0.62-0.86)	0.52 (0.28-0.70)	0.62 (0.41-0.77)	0.42 (0.16-0.62)	0.45 (0.19-0.65)
Whole Blood	0.92 (0.87-0.96)	0.93 (0.89-0.96)	0.88 (0.81-0.93)	0.95 (0.92-0.97)	0.94 (0.90-0.96)	0.41 (0.16-0.61)	0.94 (0.9-0.97)

clock estimates, we present those results in more detail in Figure 4. Specifically, we observed the strongest correlation between lung and colon using Horvath ($r=0.82$) and AltumAge ($r=0.80$) (Figure 4, top).

As expected, after adjusting for age, the inter-tissue correlations for each clock were substantially attenuated. Examining age-adjusted associations across all possible

pairs of tissue types (Supplementary Tables 3–10 and Supplementary Figures 1–6), we find evidence of weak residual correlation in clock estimates between tissues after age adjustment (Figure 3B). The means of the distributions of age-adjusted correlations for all possible tissue pairs correlations were greater than zero for each clock examined (EpiTOC $P=0.003$, Hannum $P=0.02$, Horvath $P=0.0003$, PhenoAge $P=0.01$, EpiClock $P=0.02$,

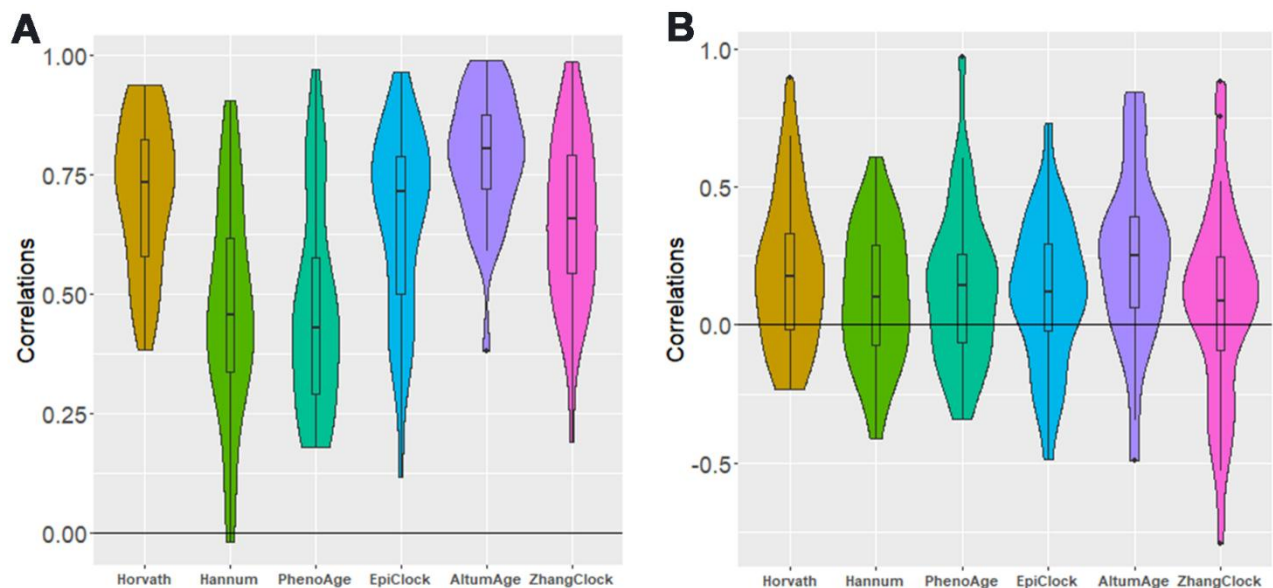


Figure 3. Distribution of between-tissue correlations for each clock, for all possible pairs of tissue types. (A) not adjusted for age (B) adjusted for age. Each of the five distributions shown (in both panels) has a mean greater than zero ($P<0.05$).

AltumAge $P < 0.001$, Zhang $P = 0.02$). Figure 4 (bottom) shows the correlation between the age-adjusted clock estimates for lung and colon, with only the Horvath clock showing a correlation with $P < 0.05$.

To assess the hypothesis that clock performance varies across tissue types due to differences in immune cell infiltration (ICI), we first examined the average leukocyte percentage in each tissue type. Based on visual inspection, there was suggestive evidence that tissue types with higher leukocyte percentage showed stronger correlation between chronological age and clock age (Supplementary Figure 7). However, given the small number of tissue types (8), we were underpowered for statistical testing, although AltumAge and EpiClock had P-values of 0.10 and 0.11, respectively.

To determine if ICI impacts clock performance, we examined with interaction between chronological age and leukocyte percentage (in relation to clock age) in a linear regression model. For some tissue types with small sample sizes (breast, kidney, muscle), the association

between chronological age and clock age was no longer clear after including the interaction ($P > 0.05$ for most clocks), suggesting lack of power for interaction testing in these tissue types (Supplementary Table 11). However, lungs showed the clearest evidence that clock performance strengthened as ICI increased, with interaction $P < 0.05$ for Horvath, Hannum, Zhang, EpiClock, PhenoAge, and EpiTOC (Supplementary Table 11).

We examined the association of participant characteristics (sex, BMI, smoking, and TL) with clock estimates for each tissue type (Supplementary Tables 12, 13). Of note, smoking showed association ($P < 0.05$) with increased DNAm clock estimates for the Horvath clock (in testis), the Hannum clock (in lung and testis), the PhenoAge clock (in lung), EpiTOC (in lung), EpiClock (in lung and testis), and AltumAge (in lung and testis) (Table 4). For the smoking analyses, 72 tests were conducted, thus the Bonferroni-corrected P-value threshold is 0.0006. PACE (blood and lung), PhenoAge (lung), and EpiClock (lung) pass this threshold.

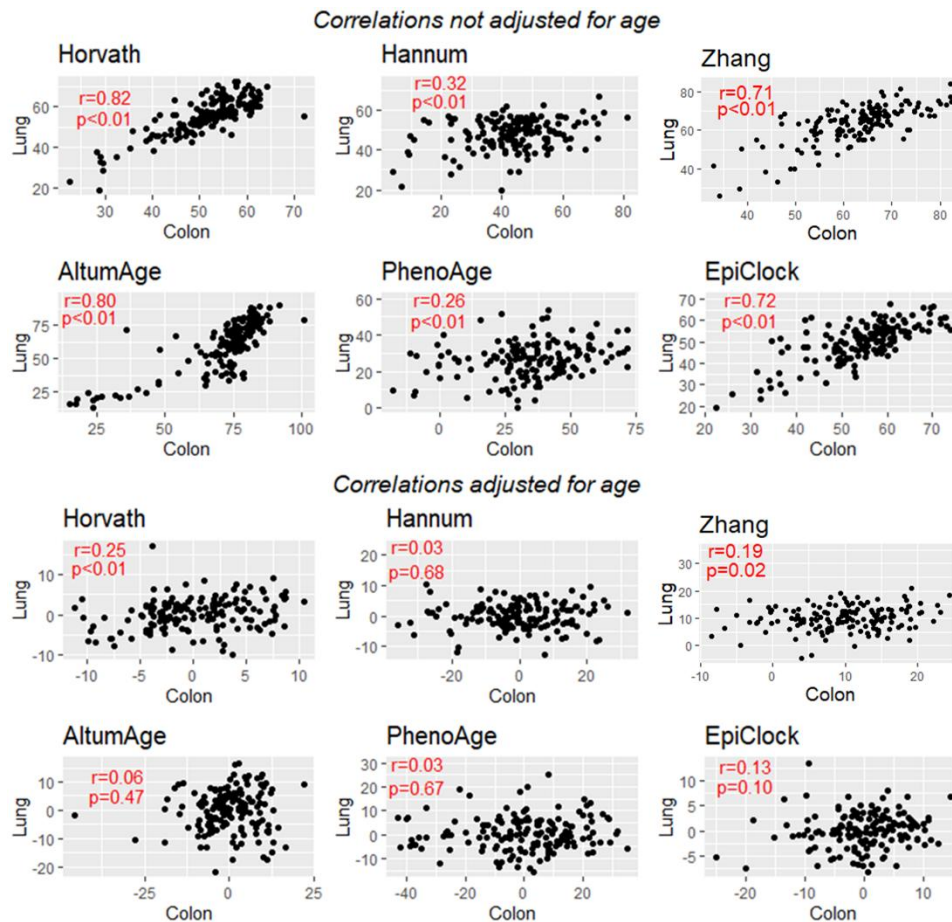


Figure 4. Correlation between lung-based and colon-based DNAm clock estimates for 6 clocks, without adjustment for age (top) and with adjustment for age (bottom). EpiTOC showed very weak evidence for correlation and is not presented.

Table 4. Beta coefficients (and P-values) for the association between smoking and age acceleration, by tissue type and clock.

	Blood (n=51)	Breast (n=36)	Colon (n=205)	Kidney (n=47)	Lung (n=194)	Muscle (n=43)	Ovary (n=142)	Prostate (n=111)	Testis (n=45)
EpiClock	3.82 (0.026)	0.02 (0.991)	-1.52 (0.128)	-0.98 (0.454)	2.00 (<0.001)	-1.96 (0.104)	0.02 (0.973)	0.12 (0.933)	5.12 (0.037)
AltumAge	6.96 (0.024)	-5.55 (0.125)	-0.69 (0.557)	-3.49 (0.071)	3.64 (0.002)	-2.22 (0.313)	2.02 (0.185)	-1.27 (0.354)	6.82 (0.103)
Horvath	3.76 (0.055)	-0.39 (0.841)	0.13 (0.328)	-4.13 (0.003)	-0.39 (0.593)	-3.34 (0.039)	1.29 (0.078)	-0.81 (0.438)	4.52 (0.032)
Hannum	1.03 (0.565)	-2.28 (0.073)	-3.43 (0.097)	-0.04 (0.738)	1.96 (0.005)	-1.83 (0.152)	-0.65 (0.339)	-1.39 (0.234)	1.23 (0.279)
PhenoAge	1.62 (0.557)	-4.20 (0.193)	-3.53 (0.20)	-1.92 (0.369)	4.92 (<0.001)	-0.97 (0.596)	0.69 (0.449)	-0.38 (0.838)	1.94 (0.205)
EpiTOC	0.00 (0.838)	-0.01 (0.241)	-0.01 (0.027)	-0.00 (0.599)	0.01 (0.003)	-0.00 (0.883)	0.00 (0.301)	0.00 (0.979)	0.00 (0.204)
Zhang	-2.32 (0.214)	-1.32 (0.339)	-2.18 (0.038)	-0.09 (0.940)	0.02 (0.980)	-3.82 (0.080)	0.01 (0.051)	-0.378 (0.221)	6.45 (0.084)
PACE	0.009 (<0.001)	0.118 (0.003)	0.064 (0.014)	0.042 (0.224)	0.083 (<0.001)	0.006 (0.805)	0.007 (0.547)	0.034 (0.222)	-0.008 (0.588)

Linear regression models include sex, BMI, and telomere length (TQI) as covariates. Association estimates with P-values <0.05 are shown in bold text. Smoking is coded as never (0) and ever (1).

DISCUSSION

In this study we have applied eight DNAm aging/clock algorithms to DNAm data derived from 9 different human tissue types, and we demonstrate that there are substantial differences in these clock estimates across tissue types. We found that the tissue types examined varied in terms of their mean clock estimates, as well as the strength of the correlation between the clock estimates and chronological age. These differences across tissue types were most apparent for clocks trained using DNAm from blood only (e.g., Hannum), but also present for clocks trained on multiple tissue types (e.g., Horvath, a clock designed for pan-tissue age prediction). When applied to different tissue types, each clock showed strong correlations of epigenetic age across tissues, but these correlations were drastically (but not completely) attenuated after adjustment for age, suggesting age acceleration estimates from a single tissue type (e.g., whole blood) can potentially serve as a proxy for other tissue types, although perhaps a weak proxy. Therefore, studies of additional tissue types are needed.

We acknowledge that some of the clocks examined here (Hannum, PhenoAge), were not developed with the goal of being applied to DNAm data from non-blood tissue types. Therefore, one should not expect these clocks to predict age (or other aging-related phenotypes) equally well across tissue types. The pan-tissue clocks tended to be better predictors of chronological age for non-blood tissues, but prediction for these clocks tended to be worse for muscle, ovary, and testis (when compared to lung,

colon, breast, kidney, and prostate). Of note, ovary and testis were not in the Horvath training sample. All clocks showed the strongest correlation with chronological age when applied to DNAm data from blood (including the pan-tissue clocks), which likely reflects the fact that blood DNAm data is the most common type of data in the datasets used to train the clocks examined in this work. Furthermore, we provide suggestive evidence that higher immune cell infiltration into non-blood tissues leads to improved clock performance. We also acknowledge that mitotic clocks, such as EpiTOC, are not designed to predict chronological age, although clear correlation with age is observed across all tissue types.

The clocks varied with respect to their mean estimate across tissues, with AltumAge tending to provide the highest age estimates and PhenoAge tending to provide the lowest age estimates. For all clocks, the mean of the clock estimate tended to be closest to mean for chronological age when applied to blood DNAm data. It is possible that some differences in performance observed among clocks may be due in part to differences in the age distribution of the clock's training dataset compared to our GTEx sample.

The effects of smoking on DNAm clock estimates appeared more pronounced in lung tissue (and perhaps in blood and testicular tissue) as compared to other tissues, with smoking being generally associated with increased DNAm aging across clocks. This observation likely reflects the fact that lung tissue is exposed to tobacco combustion products directly via inhalation,

whereas other tissue types are primarily exposed to tobacco combustion by products from the blood stream. The association of smoking with accelerated aging in testicular tissue is novel and requires validation in future studies. No other donor characteristics showed clear evidence of consistent association with clock estimates across tissue types (Supplementary Tables 12, 13).

We observed that EpiTOC estimates generally showed weaker correlations with chronological age compared to the other DNAm clocks examined. EpiTOC differs from other clocks examined here in that it is a “mitotic clock” developed to reflect the number of stem cell divisions that have occurred in a tissue’s corresponding stem cell population over time rather than being trained to predict chronological age [38].

Our results suggest that forensic applications of DNAm clocks using non-blood tissue types will provide age estimates that are not as accurate as predictions based on blood, especially if using clocks algorithms trained on blood samples. Our results also suggest that tissue-specific DNAm aging measures may have utility for detecting biological differences in organ aging, as accelerated DNAm aging due to smoking was more pronounced in lung compared to other tissue types. However, in order to draw robust conclusions regarding the consistency of association between participant characteristics and DNAm clocks across tissue types, larger samples sizes are needed.

While our study comprehensively examines how chronological age associates with epigenetic age across different tissue types using 8 DNAm clocks, there were several limitations. First, our study included some tissue types with small sample sizes (~50 samples), which limited our power to detect associations between epigenetic age and donor characteristics. Larger studies of DNAm across multiple tissue/cell types (with more metadata on donors) are needed to better understand how DNAm clocks (and individual CpG sites) relate to donor characteristics. Second, we have a limited understanding of the cell type heterogeneity of bulk tissue samples from which our DNAm data is derived. This heterogeneity may influence the performance of the clock algorithms we are studying, as we demonstrate by examining the impact of leukocyte infiltration on clock performance. Cell type deconvolution approaches have been shown to be useful for adapting blood-based clocks to perform well in other tissues, such as saliva [39]. Third, the GTEX cohort of tissue donors, all of whom were selected for inclusion in GTEX post-mortem, is strongly enriched for smokers and individuals dying at younger ages; this potential selection bias may introduce bias into the associations between epigenetic and chronological age reported in this study. Furthermore,

while our study examines DNAm clocks in nine tissue types, future studies that include additional tissue types will improve our understanding of how epigenetic aging varies across the human body.

AUTHOR CONTRIBUTIONS

M.R., C.B., and L.T. performed analyses and prepared manuscript figures. M.R. and B.L.P. interpreted the data and wrote the main manuscript text. M.G.K. and F.J. generated DNA methylation data. N.J., J.L.L., and K.D. contributed to data processing, quality control, and statistical analysis. B.L.P. conceived the project and contributed to writing/editing and data interpretation.

CONFLICTS OF INTEREST

The authors declare that they have no conflicts of interest.

FUNDING

This work was supported by grants U01 HG007601 (to B.L.P.) and R35ES028379 (to B.L.P.) and was completed in part with computational resources provided by the Center for Research Informatics at the University of Chicago. The Genotype-Tissue Expression (GTEx) Project was supported by the Common Fund of the Office of the Director of the National Institutes of Health and by NCI, NHGRI, NHLBI, NIDA, NIMH, and NINDS. We thank the donors and their families for their generous gifts of biospecimens to the GTEx research project; the Genomics Platform at the Broad Institute for data generation; F. Aguet, J. Nedzel, and K. Ardlie for sample-delivery logistics and data-release management. The founders had no role in study design, data collection and analysis, decision to publish, or preparation of the manuscript.

REFERENCES

1. López-Otín C, Blasco MA, Partridge L, Serrano M, Kroemer G. The hallmarks of aging. *Cell*. 2013; 153:1194–217. <https://doi.org/10.1016/j.cell.2013.05.039> PMID:[23746838](https://pubmed.ncbi.nlm.nih.gov/23746838/)
2. Horvath S, Raj K. DNA methylation-based biomarkers and the epigenetic clock theory of ageing. *Nat Rev Genet*. 2018; 19:371–84. <https://doi.org/10.1038/s41576-018-0004-3> PMID:[29643443](https://pubmed.ncbi.nlm.nih.gov/29643443/)
3. Ahuja N, Issa JP. Aging, methylation and cancer. *Histol Histopathol*. 2000; 15:835–42. <https://doi.org/10.14670/HH-15.835> PMID:[10963127](https://pubmed.ncbi.nlm.nih.gov/10963127/)

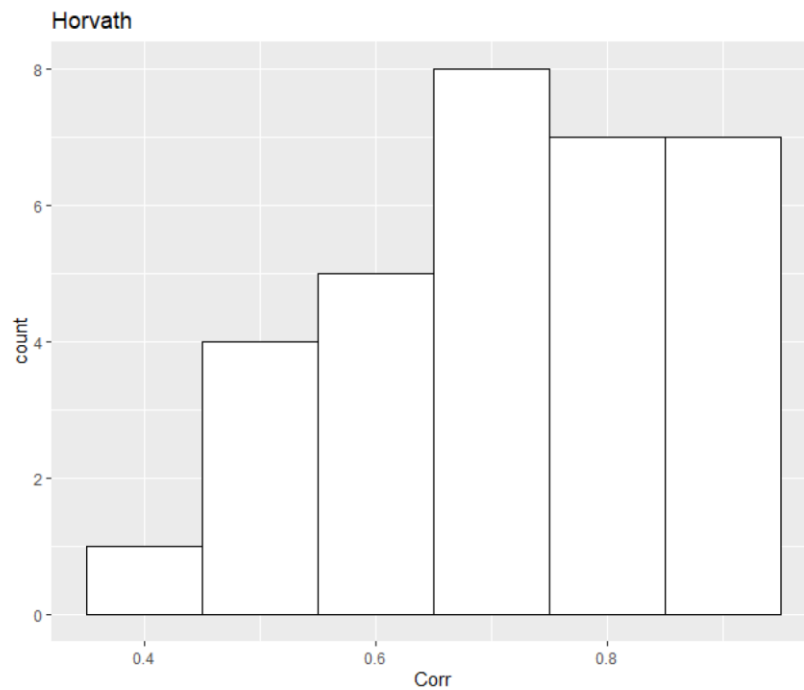
4. Toyota M, Ahuja N, Ohe-Toyota M, Herman JG, Baylin SB, Issa JP. CpG island methylator phenotype in colorectal cancer. *Proc Natl Acad Sci USA*. 1999; 96:8681–86.
<https://doi.org/10.1073/pnas.96.15.8681>
PMID:[10411935](https://pubmed.ncbi.nlm.nih.gov/10411935/)
5. Christensen BC, Houseman EA, Marsit CJ, Zheng S, Wrensch MR, Wiemels JL, Nelson HH, Karagas MR, Padbury JF, Bueno R, Sugarbaker DJ, Yeh RF, Wiencke JK, Kelsey KT. Aging and environmental exposures alter tissue-specific DNA methylation dependent upon CpG island context. *PLoS Genet*. 2009; 5:e1000602.
<https://doi.org/10.1371/journal.pgen.1000602>
PMID:[19680444](https://pubmed.ncbi.nlm.nih.gov/19680444/)
6. Maegawa S, Hinkal G, Kim HS, Shen L, Zhang L, Zhang J, Zhang N, Liang S, Donehower LA, Issa JP. Widespread and tissue specific age-related DNA methylation changes in mice. *Genome Res*. 2010; 20:332–40.
<https://doi.org/10.1101/gr.096826.109>
PMID:[20107151](https://pubmed.ncbi.nlm.nih.gov/20107151/)
7. Fraga MF, Ballestar E, Paz MF, Ropero S, Setien F, Ballestar ML, Heine-Suñer D, Cigudosa JC, Urioste M, Benitez J, Boix-Chornet M, Sanchez-Aguilera A, Ling C, et al. Epigenetic differences arise during the lifetime of monozygotic twins. *Proc Natl Acad Sci USA*. 2005; 102:10604–09.
<https://doi.org/10.1073/pnas.0500398102>
PMID:[16009939](https://pubmed.ncbi.nlm.nih.gov/16009939/)
8. Teschendorff AE, Menon U, Gentry-Maharaj A, Ramus SJ, Weisenberger DJ, Shen H, Campan M, Noushmehr H, Bell CG, Maxwell AP, Savage DA, Mueller-Holzner E, Marth C, et al. Age-dependent DNA methylation of genes that are suppressed in stem cells is a hallmark of cancer. *Genome Res*. 2010; 20:440–46.
<https://doi.org/10.1101/gr.103606.109>
PMID:[20219944](https://pubmed.ncbi.nlm.nih.gov/20219944/)
9. Rakyan VK, Down TA, Maslau S, Andrew T, Yang TP, Beyan H, Whittaker P, McCann OT, Finer S, Valdes AM, Leslie RD, Deloukas P, Spector TD. Human aging-associated DNA hypermethylation occurs preferentially at bivalent chromatin domains. *Genome Res*. 2010; 20:434–39.
<https://doi.org/10.1101/gr.103101.109>
PMID:[20219945](https://pubmed.ncbi.nlm.nih.gov/20219945/)
10. Jones MJ, Goodman SJ, Kobor MS. DNA methylation and healthy human aging. *Aging Cell*. 2015; 14:924–32.
<https://doi.org/10.1111/accel.12349> PMID:[25913071](https://pubmed.ncbi.nlm.nih.gov/25913071/)
11. Bergsma T, Rogaeva E. DNA Methylation Clocks and Their Predictive Capacity for Aging Phenotypes and Healthspan. *Neurosci Insights*. 2020; 15:2633105520942221.
<https://doi.org/10.1177/2633105520942221>
PMID:[32743556](https://pubmed.ncbi.nlm.nih.gov/32743556/)
12. Zhang W, Qu J, Liu GH, Belmonte JC. The ageing epigenome and its rejuvenation. *Nat Rev Mol Cell Biol*. 2020; 21:137–50.
<https://doi.org/10.1038/s41580-019-0204-5>
PMID:[32020082](https://pubmed.ncbi.nlm.nih.gov/32020082/)
13. Li A, Koch Z, Ideker T. Epigenetic aging: Biological age prediction and informing a mechanistic theory of aging. *J Intern Med*. 2022; 292:733–44.
<https://doi.org/10.1111/joim.13533> PMID:[35726002](https://pubmed.ncbi.nlm.nih.gov/35726002/)
14. Lu AT, Quach A, Wilson JG, Reiner AP, Aviv A, Raj K, Hou L, Baccarelli AA, Li Y, Stewart JD, Whitsel EA, Assimes TL, Ferrucci L, Horvath S. DNA methylation GrimAge strongly predicts lifespan and healthspan. *Aging (Albany NY)*. 2019; 11:303–27.
<https://doi.org/10.18632/aging.101684>
PMID:[30669119](https://pubmed.ncbi.nlm.nih.gov/30669119/)
15. Levine ME, Lu AT, Quach A, Chen BH, Assimes TL, Bandinelli S, Hou L, Baccarelli AA, Stewart JD, Li Y, Whitsel EA, Wilson JG, Reiner AP, et al. An epigenetic biomarker of aging for lifespan and healthspan. *Aging (Albany NY)*. 2018; 10:573–91.
<https://doi.org/10.18632/aging.101414>
PMID:[29676998](https://pubmed.ncbi.nlm.nih.gov/29676998/)
16. Yang Z, Wong A, Kuh D, Paul DS, Rakyan VK, Leslie RD, Zheng SC, Widschwendter M, Beck S, Teschendorff AE. Correlation of an epigenetic mitotic clock with cancer risk. *Genome Biol*. 2016; 17:205.
<https://doi.org/10.1186/s13059-016-1064-3>
PMID:[27716309](https://pubmed.ncbi.nlm.nih.gov/27716309/)
17. Vijayakumar KA, Cho GW. Pan-tissue methylation aging clock: Recalibrated and a method to analyze and interpret the selected features. *Mech Ageing Dev*. 2022; 204:111676.
<https://doi.org/10.1016/j.mad.2022.111676>
PMID:[35489615](https://pubmed.ncbi.nlm.nih.gov/35489615/)
18. de Lima Camillo LP, Lapierre LR, Singh R. A pan-tissue DNA-methylation epigenetic clock based on deep learning. *NPJ Aging*. 2022; 8:4.
19. Zhang Q, Vallerga CL, Walker RM, Lin T, Henders AK, Montgomery GW, He J, Fan D, Fowdar J, Kennedy M, Pitcher T, Pearson J, Halliday G, et al. Improved precision of epigenetic clock estimates across tissues and its implication for biological ageing. *Genome Med*. 2019; 11:54.
<https://doi.org/10.1186/s13073-019-0667-1>
PMID:[31443728](https://pubmed.ncbi.nlm.nih.gov/31443728/)
20. Belsky DW, Caspi A, Corcoran DL, Sugden K, Poulton R, Arseneault L, Baccarelli A, Chamarti K, Gao X, Hannon E, Harrington HL, Houts R, Kothari M, et al. DunedinPACE, a DNA methylation biomarker of the pace of aging. *Elife*. 2022; 11:e73420.
<https://doi.org/10.7554/eLife.73420> PMID:[35029144](https://pubmed.ncbi.nlm.nih.gov/35029144/)

21. Grodstein F, Lemos B, Yu L, Iatrou A, De Jager PL, Bennett DA. Characteristics of Epigenetic Clocks Across Blood and Brain Tissue in Older Women and Men. *Front Neurosci.* 2021; 14:555307. <https://doi.org/10.3389/fnins.2020.555307> PMID:[33488342](https://pubmed.ncbi.nlm.nih.gov/33488342/)
22. Bell CG, Lowe R, Adams PD, Baccarelli AA, Beck S, Bell JT, Christensen BC, Gladyshev VN, Heijmans BT, Horvath S, Ideker T, Issa JJ, Kelsey KT, et al. DNA methylation aging clocks: challenges and recommendations. *Genome Biol.* 2019; 20:249. <https://doi.org/10.1186/s13059-019-1824-y> PMID:[31767039](https://pubmed.ncbi.nlm.nih.gov/31767039/)
23. GTEx Consortium. The Genotype-Tissue Expression (GTEx) project. *Nat Genet.* 2013; 45:580–85. <https://doi.org/10.1038/ng.2653> PMID:[23715323](https://pubmed.ncbi.nlm.nih.gov/23715323/)
24. GTEx Consortium. The GTEx Consortium atlas of genetic regulatory effects across human tissues. *Science.* 2020; 369:1318–30. <https://doi.org/10.1126/science.aaz1776> PMID:[32913098](https://pubmed.ncbi.nlm.nih.gov/32913098/)
25. GTEx Portal [Internet]. 2022. <https://www.gtexportal.org/home/>
26. eGTEx Project. Enhancing GTEx by bridging the gaps between genotype, gene expression, and disease. *Nat Genet.* 2017; 49:1664–70. <https://doi.org/10.1038/ng.3969> PMID:[29019975](https://pubmed.ncbi.nlm.nih.gov/29019975/)
27. Oliva M, Demanelis K, Lu Y, Chernoff M, Jasmine F, Ahsan H, Kibriya MG, Chen LS, Pierce BL. DNA methylation QTL mapping across diverse human tissues provides molecular links between genetic variation and complex traits. *Nat Genet.* 2023; 55:112–22. <https://doi.org/10.1038/s41588-022-01248-z> PMID:[36510025](https://pubmed.ncbi.nlm.nih.gov/36510025/)
28. Morris TJ, Butcher LM, Feber A, Teschendorff AE, Chakravarthy AR, Wojdacz TK, Beck S. ChAMP: 450k Chip Analysis Methylation Pipeline. *Bioinformatics.* 2014; 30:428–30. <https://doi.org/10.1093/bioinformatics/btt684> PMID:[24336642](https://pubmed.ncbi.nlm.nih.gov/24336642/)
29. Triche TJ Jr, Weisenberger DJ, Van Den Berg D, Laird PW, Siegmund KD. Low-level processing of Illumina Infinium DNA Methylation BeadArrays. *Nucleic Acids Res.* 2013; 41:e90. <https://doi.org/10.1093/nar/gkt090> PMID:[23476028](https://pubmed.ncbi.nlm.nih.gov/23476028/)
30. Fortin JP, Triche TJ Jr, Hansen KD. Preprocessing, normalization and integration of the Illumina HumanMethylationEPIC array with minfi. *Bioinformatics.* 2017; 33:558–60. <https://doi.org/10.1093/bioinformatics/btw691> PMID:[28035024](https://pubmed.ncbi.nlm.nih.gov/28035024/)
31. Teschendorff AE, Marabita F, Lechner M, Bartlett T, Tegner J, Gomez-Cabrero D, Beck S. A beta-mixture quantile normalization method for correcting probe design bias in Illumina Infinium 450 k DNA methylation data. *Bioinformatics.* 2013; 29:189–96. <https://doi.org/10.1093/bioinformatics/bts680> PMID:[23175756](https://pubmed.ncbi.nlm.nih.gov/23175756/)
32. Home | DNA Methylation Age Calculator [Internet]. 2023. <https://dnamage.genetics.ucla.edu/>
33. Horvath S. DNA methylation age of human tissues and cell types. *Genome Biol.* 2013; 14:R115. <https://doi.org/10.1186/gb-2013-14-10-r115> PMID:[24138928](https://pubmed.ncbi.nlm.nih.gov/24138928/)
34. AltumAge [Internet]. Singh Lab @ Brown. 2023. <https://github.com/rsinghlab/AltumAge>
35. Hannum G, Guinney J, Zhao L, Zhang L, Hughes G, Sada S, Klotzle B, Bibikova M, Fan JB, Gao Y, Deconde R, Chen M, Rajapakse I, et al. Genome-wide methylation profiles reveal quantitative views of human aging rates. *Mol Cell.* 2013; 49:359–67. <https://doi.org/10.1016/j.molcel.2012.10.016> PMID:[23177740](https://pubmed.ncbi.nlm.nih.gov/23177740/)
36. Aran D, Sirota M, Butte AJ. Systematic pan-cancer analysis of tumour purity. *Nat Commun.* 2015; 7:10707. <https://doi.org/10.1038/ncomms9971> PMID:[26634437](https://pubmed.ncbi.nlm.nih.gov/26634437/)
37. Demanelis K, Jasmine F, Chen LS, Chernoff M, Tong L, Delgado D, Zhang C, Shinkle J, Sabarinathan M, Lin H, Ramirez E, Oliva M, Kim-Hellmuth S, et al, and GTEx Consortium. Determinants of telomere length across human tissues. *Science.* 2020; 369:eaaz6876. <https://doi.org/10.1126/science.aaz6876> PMID:[32913074](https://pubmed.ncbi.nlm.nih.gov/32913074/)
38. Teschendorff AE. A comparison of epigenetic mitotic-like clocks for cancer risk prediction. *Genome Med.* 2020; 12:56. <https://doi.org/10.1186/s13073-020-00752-3> PMID:[32580750](https://pubmed.ncbi.nlm.nih.gov/32580750/)
39. Galkin F, Kochetov K, Mamoshina P, Zhavoronkov A. Adapting Blood DNA Methylation Aging Clocks for Use in Saliva Samples With Cell-type Deconvolution. *Front Aging.* 2021; 2:697254. <https://doi.org/10.3389/fragi.2021.697254> PMID:[35822029](https://pubmed.ncbi.nlm.nih.gov/35822029/)

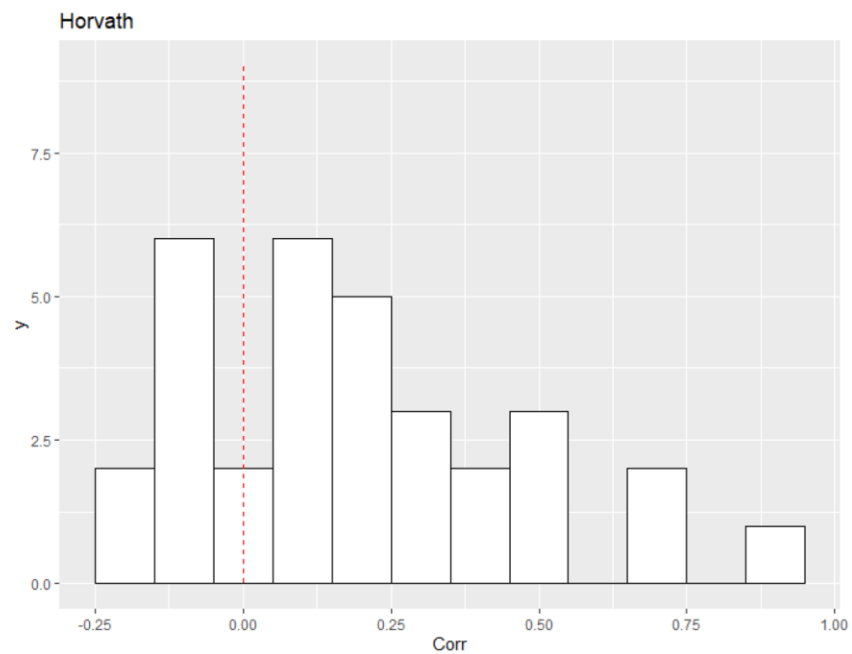
SUPPLEMENTARY MATERIALS

Supplementary Figures

A (not age-adjusted)

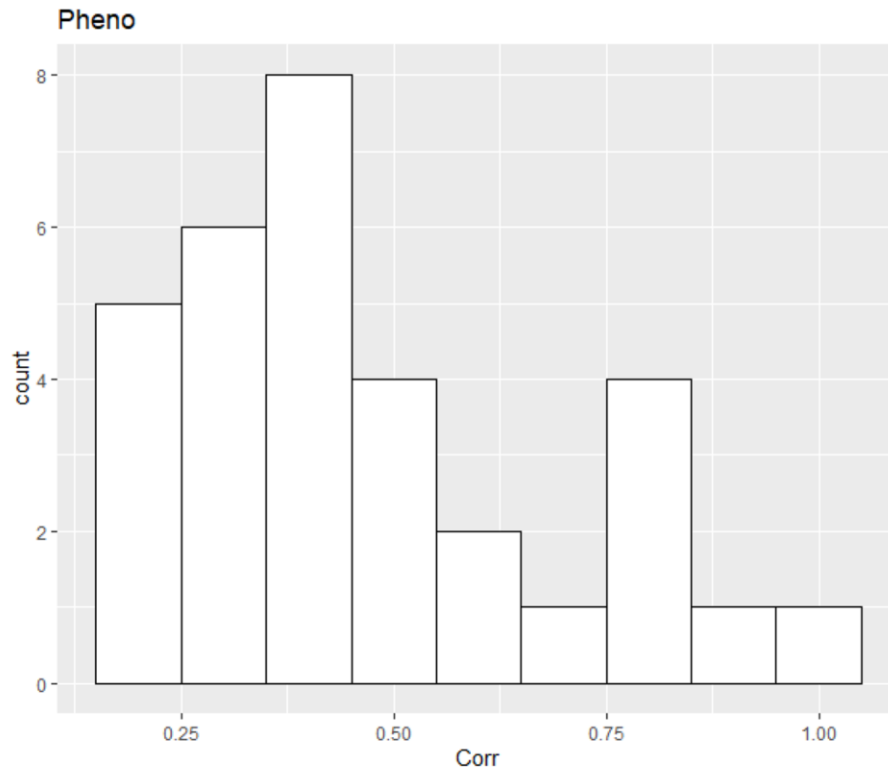


B (age-adjusted)

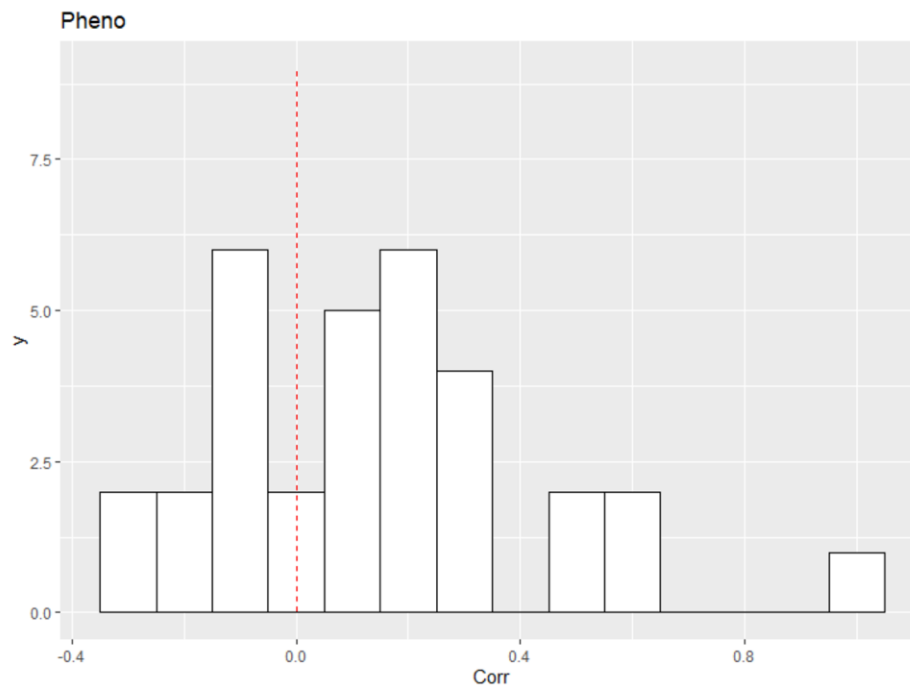


Supplementary Figure 1. Distribution of Correlation Estimates (from Supplementary Table 3) for all Tissue pairs for the Horvath Clock (A), not age-adjusted; (B) age-adjusted.

A(not age adjusted)

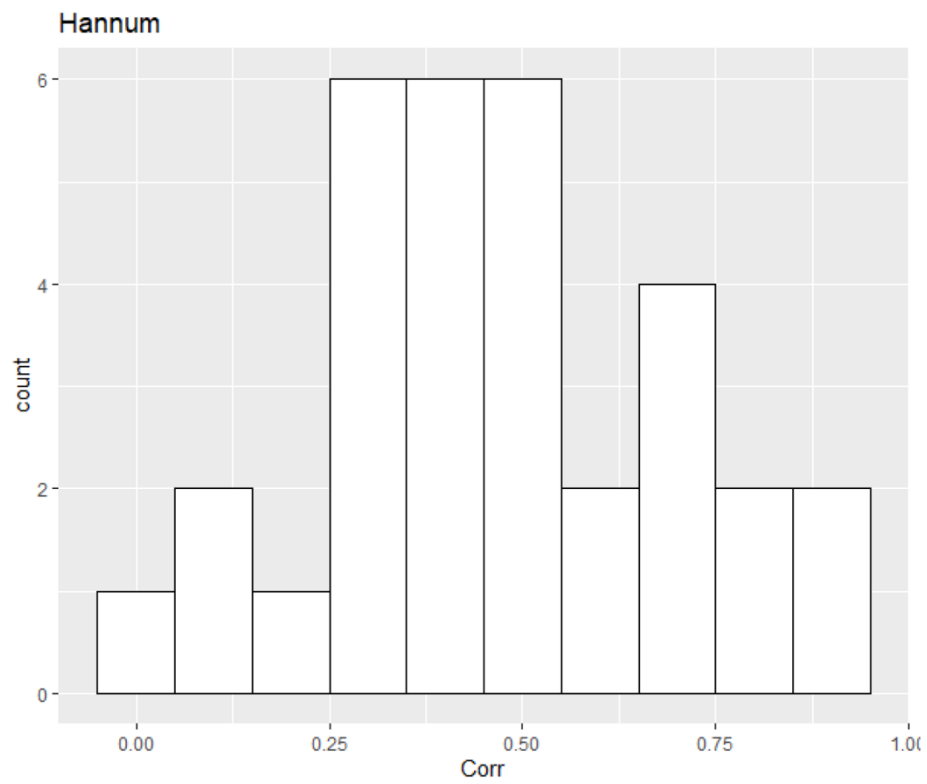


B(age-adjusted)

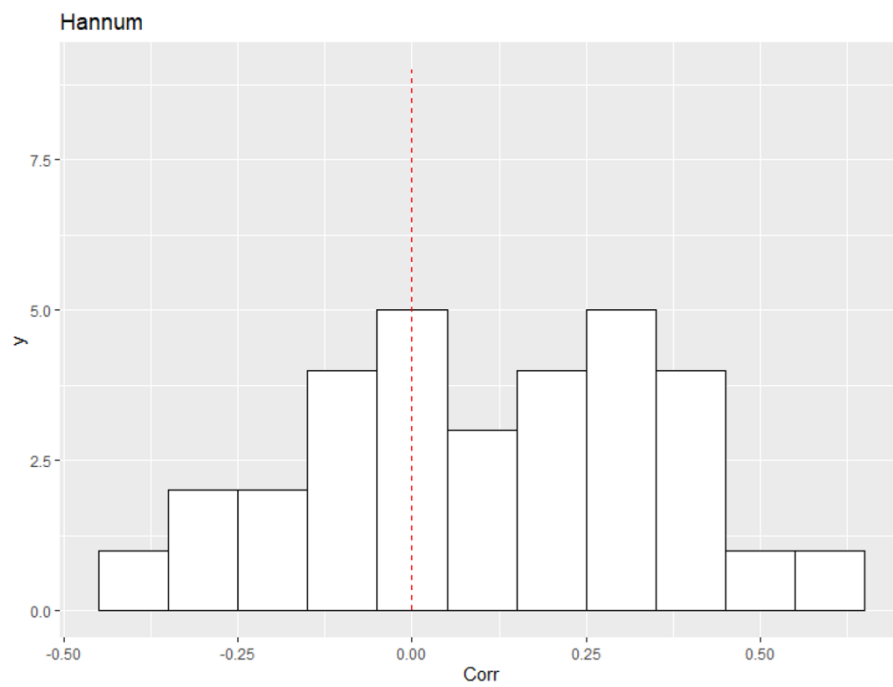


Supplementary Figure 2. Distribution of Correlation Estimates (from Supplementary Table 4) for all Tissue pairs for the PhenoAge Clock (A), not age-adjusted; (B) age-adjusted.

A (not age-adjusted)

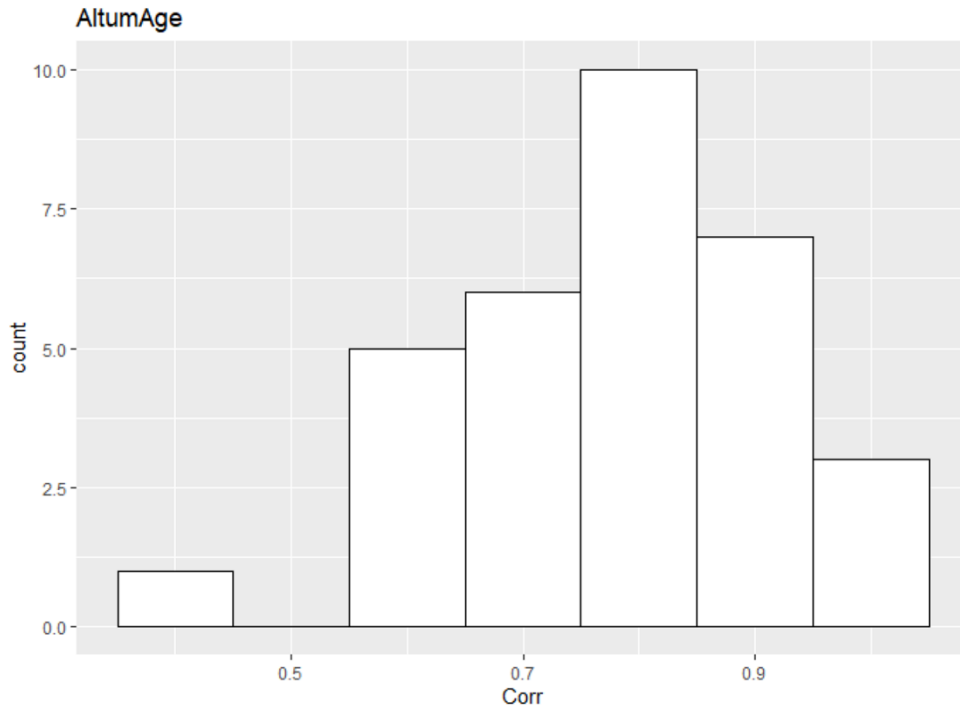


B (age adjusted)

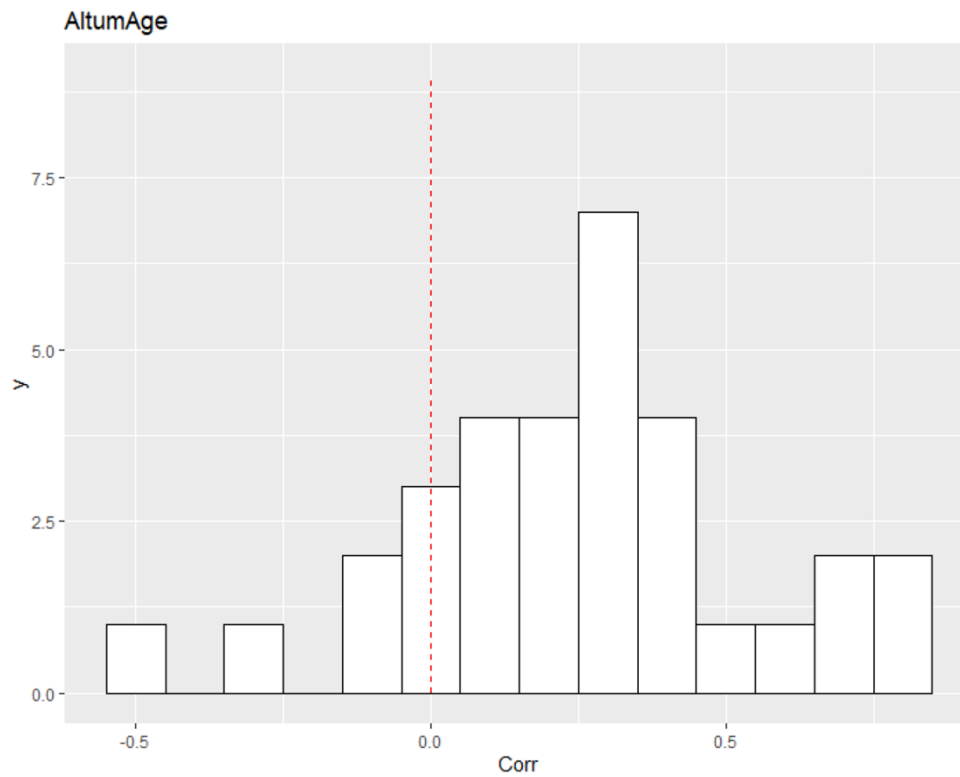


Supplementary Figure 3. Distribution of Correlation Estimates (from Supplementary Table 5) for all Tissue pairs for the Hannum Clock (**A**), not age-adjusted; (**B**) age-adjusted.

A (not age-adjusted)

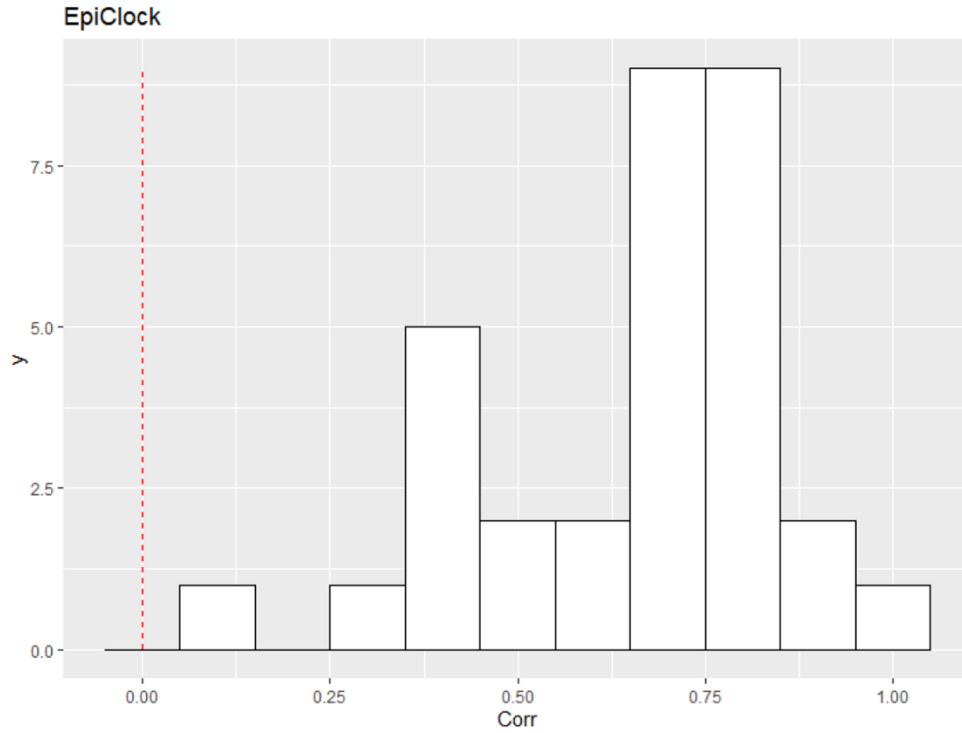


B (age-adjusted)

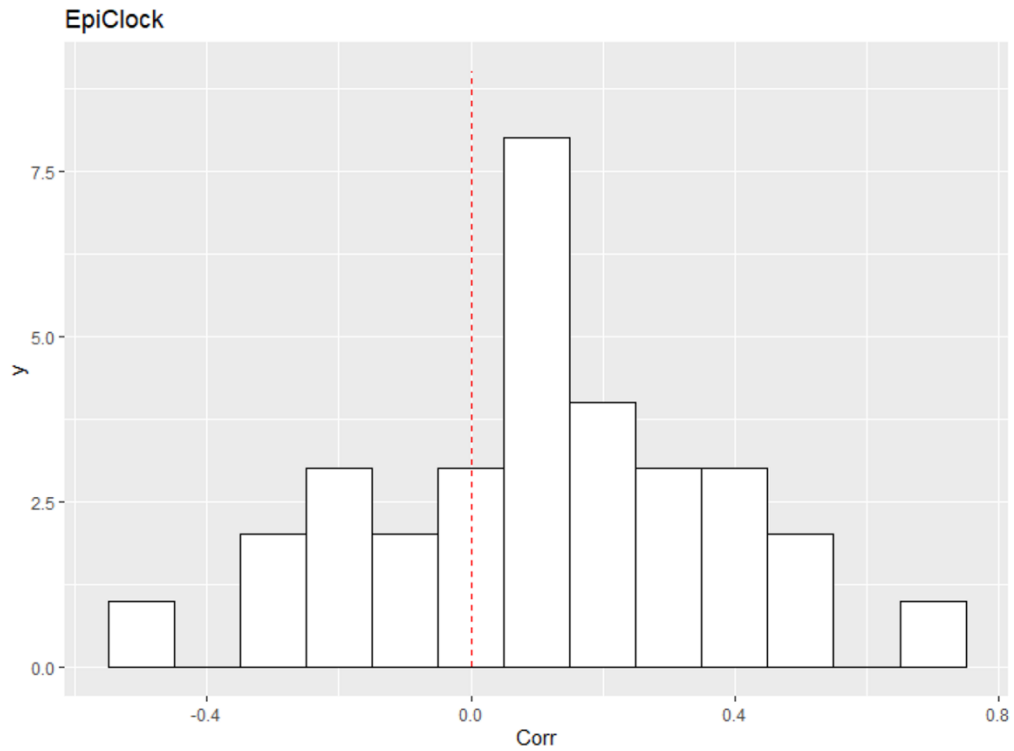


Supplementary Figure 4. Distribution of Correlation Estimates (from Supplementary Table 6) for all Tissue pairs for the AltumAge Clock (A), not age-adjusted; (B) age-adjusted.

A (not age-adjusted)

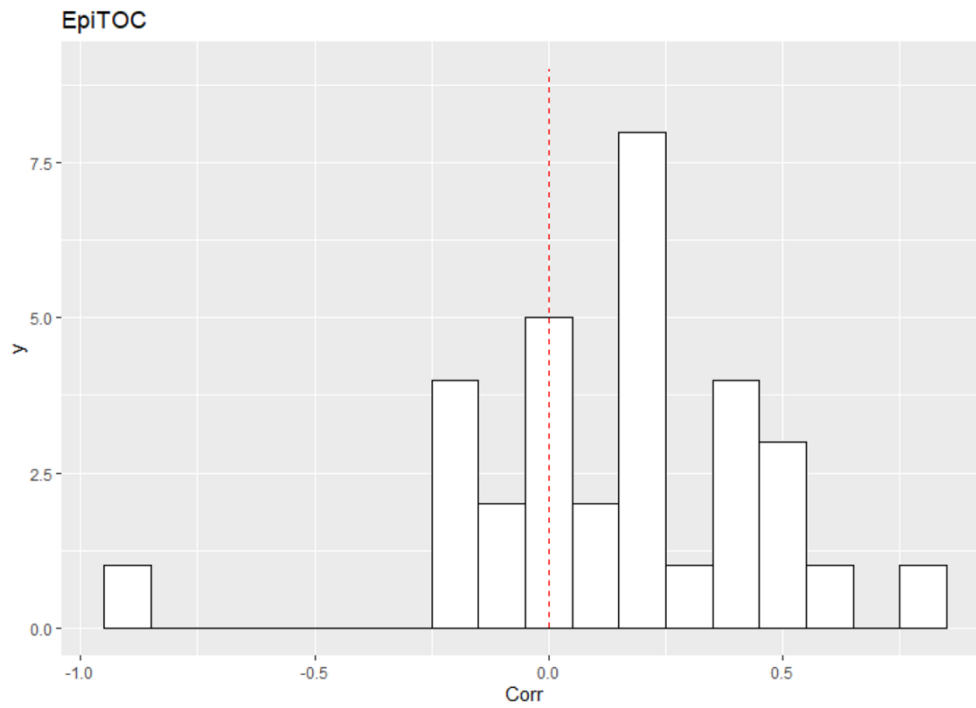


B (age-adjusted)

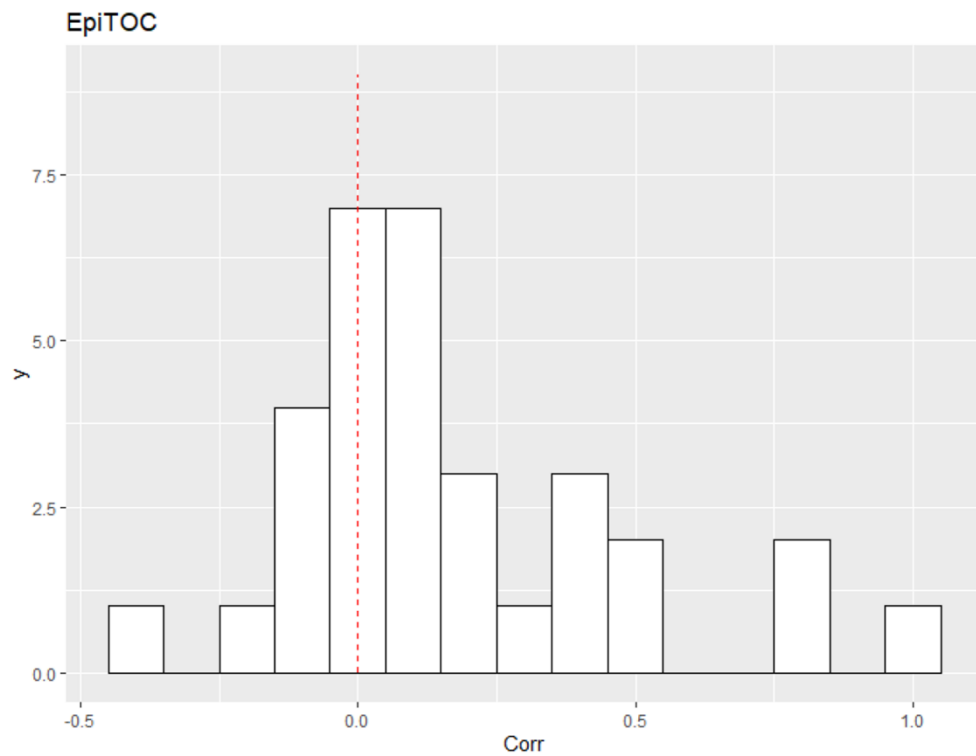


Supplementary Figure 5. Distribution of Correlation Estimates (from Supplementary Table 7) for all Tissue pairs for EpiClock (A), not age-adjusted; (B) age-adjusted.

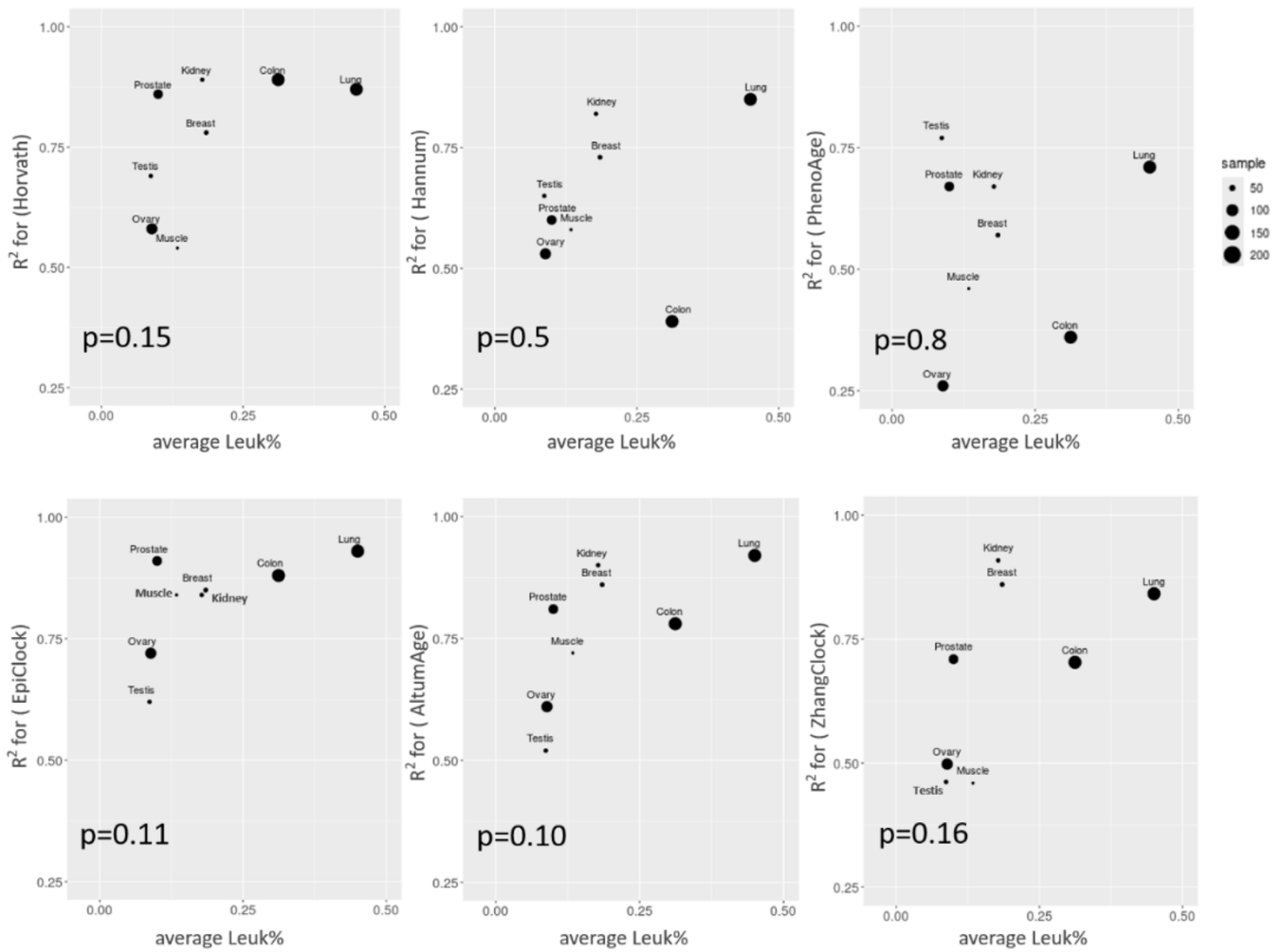
A (not age-adjusted)



B (age-adjusted)



Supplementary Figure 6. Distribution of Correlation Estimates (from Supplementary Table 8) for all Tissue pairs for EpiTOC (A), not age-adjusted; (B) age-adjusted.



Supplementary Figure 7. Scatter plot of average leukocyte percentage (from LUMP) vs. the R² for each clock's association with chronological age. P-values correspond to the association between leukocyte percentage and the R² value (n=8).

Supplementary Tables

Please browse Full Text version to see the data of Supplementary Table 11.

Supplementary Table 1. Median absolute error/difference for each clock, by tissue type.

Clock	Breast	Colon	Kidney	Lung	Muscle	Ovary	Prostate	Testis	Blood
AltumAge	16.17	17.72	22.49	10.51	14.17	6.333	12.65	14.26	13.51
Horvath	3.524	4.974	3.375	3.991	14.72	25.56	4.732	20.38	2.976
PhenoAge	23.63	21.26	38.27	29.98	55.50	60.87	30.40	43.86	4.807
EpiClock	8.644	4.564	9.766	5.655	15.93	23.07	10.89	29.12	2.607
Hannum	22.07	13.66	18.44	7.733	41.20	39.54	20.44	43.08	5.198
Zhang	4.534	7.177	2.781	7.814	18.43	14.57	7.647	29.36	2.016

Supplementary Table 2. Average age acceleration (mean deviation) for each clock, by tissue type.

Clock	Blood	Breast	Colon	Kidney	Lung	Muscle	Ovary	Prostate	Testes
Horvath	-1.56	0.85	-4.75	-2.63	-0.20	-13.45	-23.74	0.05	-18.58
Altum	9.12	14.89	15.94	23.11	4.73	13.16	-0.36	12.09	-10.82
EpiClock	2.01	-8.65	-1.07	-9.74	-5.57	-14.01	-21.44	-10.23	-28.06
Hannum	-4.38	-21.29	-11.90	-18.33	-7.63	-40.77	-37.34	-18.17	-41.21
PhenoAge	-0.17	-23.80	-21.32	-38.07	-29.67	-54.79	-59.12	-30.42	-44.06
Zhang	0.22	-2.96	7.24	-2.10	7.70	-18.17	-12.79	-6.26	-29.20

Supplementary Table 3. Correlation between tissue types for the Horvath clock.

Non-adjusted correlation	Age-adjusted correlation	Tissue type pair	Sample size	Chronological age range
0.769	0.249	Breast Colon	15	21-70
0.927	-0.115	Breast Kidney	5	42-66
0.656	0.231	Breast Lung	16	37-70
0.938	0.894	Breast Muscle	4	40-66
0.809	0.248	Breast Ovary	28	21-69
0.871	-0.065	Breast Blood	5	42-66
0.731	0.211	Colon Kidney	38	36-70
0.819	0.254	Colon Lung	153	22-70
0.573	-0.051	Colon Muscle	28	31-70
0.457	-0.065	Colon Ovary	53	21-70
0.842	0.223	Colon Prostate	85	22-70
0.682	0.111	Colon Testis	38	22-70
0.924	0.532	Colon Blood	45	22-70
0.724	0.438	Kidney Lung	26	39-68
0.893	0.684	Kidney Muscle	12	42-70
0.738	0.656	Kidney Ovary	11	42-68
0.771	0.303	Kidney Prostate	30	36-70
0.384	-0.234	Kidney Testis	27	36-70
0.721	0.101	Kidney Blood	24	36-70
0.557	0.111	Lung Muscle	25	31-67
0.469	-0.125	Lung Ovary	51	22-70
0.789	0.132	Lung Prostate	73	22-70
0.476	0.058	Lung Testis	33	25-68
0.897	0.546	Lung Blood	37	22-68
0.635	0.377	Muscle Ovary	12	34-70
0.761	0.461	Muscle Prostate	16	31-70
0.475	0.028	Muscle Testis	11	31-70
0.742	-0.004	Muscle Blood	11	31-70
0.581	-0.148	Ovary Blood	9	42-66
0.576	-0.201	Prostate Testis	39	22-70
0.893	0.317	Prostate Blood	33	22-70
0.671	0.145	Testis Blood	27	22-70

Supplementary Table 4. Correlation between tissue types for the PhenoAge clock.

Non-adjusted correlation	Age-adjusted correlation	Tissue type pair	Sample size	Chronological age range
0.483	0.338	Breast Colon	15	21-70
0.852	0.556	Breast Kidney	5	42-66
0.179	-0.341	Breast Lung	16	37-70
0.971	0.971	Breast Muscle	4	40-66
0.305	0.144	Breast Ovary	28	21-69
0.435	-0.206	Breast Blood	5	42-66
0.411	0.072	Colon Kidney	38	36-70
0.259	0.035	Colon Lung	153	22-70
0.299	0.241	Colon Muscle	28	31-70
0.221	0.185	Colon Ovary	53	21-70
0.266	-0.046	Colon Prostate	85	22-70
0.328	-0.149	Colon Testis	38	22-70
0.479	0.189	Colon Blood	45	22-70
0.185	-0.197	Kidney Lung	26	39-68
0.424	-0.126	Kidney Muscle	12	42-70
0.231	-0.281	Kidney Ovary	11	42-68
0.448	0.142	Kidney Prostate	30	36-70
0.423	-0.099	Kidney Testis	27	36-70
0.522	-0.056	Kidney Blood	24	36-70
0.426	0.151	Lung Muscle	25	31-67
0.218	0.056	Lung Ovary	51	22-70
0.415	-0.085	Lung Prostate	73	22-70
0.563	0.219	Lung Testis	33	25-68
0.777	0.476	Lung Blood	37	22-68
0.271	0.261	Muscle Ovary	12	34-70
0.449	0.243	Muscle Prostate	16	31-70
0.791	0.341	Muscle Testis	11	31-70
0.801	0.474	Muscle Blood	11	31-70
0.615	0.601	Ovary Blood	9	42-66
0.533	-0.058	Prostate Testis	39	22-70
0.724	0.069	Prostate Blood	33	22-70
0.801	0.251	Testis Blood	27	22-70

Supplementary Table 5. Correlation between tissue types for the Hannum clock.

Non-adjusted correlation	Age-adjusted correlation	Tissue type pair	Sample size	Chronological age range
0.417	0.152	Breast Colon	15	21-70
0.881	0.606	Breast Kidney	5	42-66
0.489	-0.084	Breast Lung	16	37-70
0.066	0.338	Breast Muscle	4	40-66
0.479	0.271	Breast Ovary	28	21-69
0.654	0.183	Breast Blood	5	42-66
0.729	0.439	Colon Kidney	38	36-70
0.318	0.034	Colon Lung	153	22-70
0.433	0.391	Colon Muscle	28	31-70
0.109	-0.014	Colon Ovary	53	21-70
0.381	0.095	Colon Prostate	85	22-70
0.266	-0.181	Colon Testis	38	22-70
0.532	0.274	Colon Blood	45	22-70
0.493	0.017	Kidney Lung	26	39-68
0.541	-0.071	Kidney Muscle	12	42-70
0.337	-0.159	Kidney Ovary	11	42-68
0.414	-0.041	Kidney Prostate	30	36-70
0.422	-0.042	Kidney Testis	27	36-70
0.743	0.108	Kidney Blood	24	36-70
0.606	0.327	Lung Muscle	25	31-67
0.336	-0.251	Lung Ovary	51	22-70
0.579	0.0899	Lung Prostate	73	22-70
0.391	-0.129	Lung Testis	33	25-68
0.905	0.462	Lung Blood	37	22-68
0.191	0.178	Muscle Ovary	12	34-70
0.512	0.391	Muscle Prostate	16	31-70
0.337	-0.109	Muscle Testis	11	31-70
0.695	0.153	Muscle Blood	11	31-70
-0.018	-0.412	Ovary Blood	9	42-66
0.314	-0.268	Prostate Testis	39	22-70
0.766	0.261	Prostate Blood	33	22-70
0.767	0.396	Testis Blood	27	22-70

Supplementary Table 6. Correlation between tissue types for the AltumAge clock.

Non-adjusted correlation	Age-adjusted correlation	Tissue type pair	Sample size	Chronological age range
0.774	0.252	Breast Colon	15	21-70
0.991	0.711	Breast Kidney	5	42-66
0.711	0.074	Breast Lung	16	37-70
0.957	0.844	Breast Muscle	4	40-66
0.724	0.222	Breast Ovary	28	21-69
0.868	-0.493	Breast Blood	5	42-66
0.861	0.518	Colon Kidney	38	36-70
0.792	0.059	Colon Lung	153	22-70
0.811	0.347	Colon Muscle	28	31-70
0.591	0.064	Colon Ovary	53	21-70
0.896	0.343	Colon Prostate	85	22-70
0.608	0.035	Colon Testis	38	22-70
0.963	0.395	Colon Blood	45	22-70
0.752	0.383	Kidney Lung	26	39-68
0.935	0.841	Kidney Muscle	12	42-70
0.728	0.393	Kidney Ovary	11	42-68
0.811	0.266	Kidney Prostate	30	36-70
0.382	-0.111	Kidney Testis	27	36-70
0.837	0.201	Kidney Blood	24	36-70
0.804	0.167	Lung Muscle	25	31-67
0.676	-0.141	Lung Ovary	51	22-70
0.831	-0.009	Lung Prostate	73	22-70
0.647	0.324	Lung Testis	33	25-68
0.949	0.639	Lung Blood	37	22-68
0.929	0.703	Muscle Ovary	12	34-70
0.848	0.181	Muscle Prostate	16	31-70
0.648	0.251	Muscle Testis	11	31-70
0.806	0.397	Muscle Blood	11	31-70
0.743	-0.344	Ovary Blood	9	42-66
0.632	-0.042	Prostate Testis	39	22-70
0.908	0.062	Prostate Blood	33	22-70
0.749	0.319	Testis Blood	27	22-70

Supplementary Table 7. Correlation between tissue types for EpiClock.

Non-adjusted correlation	Age-adjusted correlation	Tissue type pair	Sample size	Chronological age range
0.834	0.414	Breast Colon	15	21-70
0.836	-0.221	Breast Kidney	5	42-66
0.758	-0.084	Breast Lung	16	37-70
0.786	0.423	Breast Muscle	4	40-66
0.725	0.308	Breast Ovary	28	21-69
0.772	-0.485	Breast Blood	5	42-66
0.751	0.141	Colon Kidney	38	36-70
0.717	0.131	Colon Lung	153	22-70
0.555	0.235	Colon Muscle	28	31-70
0.329	-0.152	Colon Ovary	53	21-70
0.713	0.122	Colon Prostate	85	22-70
0.507	0.069	Colon Testis	38	22-70
0.857	0.093	Colon Blood	45	22-70
0.799	0.467	Kidney Lung	26	39-68
0.681	0.315	Kidney Muscle	12	42-70
0.378	-0.286	Kidney Ovary	11	42-68
0.659	0.211	Kidney Prostate	30	36-70
0.392	0.064	Kidney Testis	27	36-70
0.891	0.457	Kidney Blood	24	36-70
0.746	0.213	Lung Muscle	25	31-67
0.449	-0.301	Lung Ovary	51	22-70
0.732	0.044	Lung Prostate	73	22-70
0.367	-0.129	Lung Testis	33	25-68
0.964	0.731	Lung Blood	37	22-68
0.667	0.001	Muscle Ovary	12	34-70
0.611	0.291	Muscle Prostate	16	31-70
0.444	0.033	Muscle Testis	11	31-70
0.828	0.394	Muscle Blood	11	31-70
0.116	-0.239	Ovary Blood	9	42-66
0.476	0.083	Prostate Testis	39	22-70
0.844	0.121	Prostate Blood	33	22-70
0.681	0.244	Testis Blood	27	22-70

Supplementary Table 8. Correlation between tissue types for the EpiTOC clock.

Non-adjusted correlation	Age-adjusted correlation	Tissue type pair	Sample size	Chronological age range
0.072	-0.034	Breast Colon	15	21-70
0.191	0.046	Breast Kidney	5	42-66
-0.074	0.073	Breast Lung	16	37-70
-0.867	0.463	Breast Muscle	4	40-66
-0.086	0.318	Breast Ovary	28	21-69
0.844	0.833	Breast Blood	5	42-66
0.245	-0.035	Colon Kidney	38	36-70
0.161	0.031	Colon Lung	153	22-70
0.034	0.057	Colon Muscle	28	31-70
-0.162	-0.167	Colon Ovary	53	21-70
0.169	-0.039	Colon Prostate	85	22-70
0.287	-0.356	Colon Testis	38	22-70
0.413	0.191	Colon Blood	45	22-70
0.379	0.368	Kidney Lung	26	39-68
-0.008	-0.057	Kidney Muscle	12	42-70
0.471	-0.069	Kidney Ovary	11	42-68
0.178	0.109	Kidney Prostate	30	36-70
0.437	0.237	Kidney Testis	27	36-70
0.461	0.421	Kidney Blood	24	36-70
-0.009	0.044	Lung Muscle	25	31-67
0.176	0.401	Lung Ovary	51	22-70
0.134	0.101	Lung Prostate	73	22-70
-0.155	0.155	Lung Testis	33	25-68
0.541	0.531	Lung Blood	37	22-68
-0.168	0.953	Muscle Ovary	12	34-70
-0.249	0.071	Muscle Prostate	16	31-70
0.571	0.775	Muscle Testis	11	31-70
0.395	-0.087	Muscle Blood	11	31-70
0.245	0.073	Ovary Blood	9	42-66
-0.021	-0.082	Prostate Testis	39	22-70
0.218	0.092	Prostate Blood	33	22-70
-0.044	-0.038	Testis Blood	27	22-70

Supplementary Table 9. Correlation between tissue types for the Zhang clock.

Non-adjusted correlation	Age-adjusted correlation	Tissue type pair	Sample size	Chronological age range
0.662	0.043	Breast Colon	15	21-70
0.851	0.260	Breast Kidney	5	42-66
0.830	0.048	Breast Lung	16	37-70
0.988	0.882	Breast Muscle	4	40-66
0.777	0.447	Breast Ovary	28	21-69
0.723	-0.416	Breast Blood	5	42-66
0.785	0.246	Colon Kidney	38	36-70
0.713	0.185	Colon Lung	152	22-70
0.640	0.399	Colon Muscle	28	31-70
0.375	0.045	Colon Ovary	50	21-70
0.565	0.041	Colon Prostate	85	22-70
0.552	0.046	Colon Testis	38	22-70
0.855	0.097	Colon Blood	45	22-70
0.810	0.362	Kidney Lung	26	39-68
0.738	0.188	Kidney Muscle	12	42-70
0.451	-0.179	Kidney Ovary	11	42-68
0.590	0.172	Kidney Prostate	30	36-70
0.462	0.079	Kidney Testis	27	36-70
0.879	0.244	Kidney Blood	24	36-70
0.654	0.010	Lung Muscle	25	31-67
0.643	-0.268	Lung Ovary	48	22-70
0.491	-0.400	Lung Prostate	73	22-70
0.446	-0.066	Lung Testis	33	25-68
0.929	0.518	Lung Blood	37	22-68
0.550	0.753	Muscle Ovary	12	34-70
0.660	0.234	Muscle Prostate	16	31-70
0.467	0.110	Muscle Testis	11	31-70
0.830	-0.531	Muscle Blood	11	31-70
0.192	-0.790	Ovary Blood	9	42-66
0.523	0.167	Prostate Testis	38	22-70
0.556	-0.340	Prostate Blood	33	22-70
0.684	-0.253	Testis Blood	27	22-70

Supplementary Table 10. Correlation between tissue types for DunedinPACE clock estimates.

Non-adjusted correlation	Pair	Sample size	Chronological age range
0.011	Breast Colon	15	21-70
0.509	Breast Kidney	5	42-66
0.424	Breast Lung	16	37-70
0.526	Breast Muscle	4	40-66
0.298	Breast Ovary	28	21-69
0.336	Breast Blood	5	42-66
0.358	Colon Kidney	38	36-70
0.138	Colon Lung	153	22-70
0.332	Colon Muscle	28	31-70
-0.160	Colon Ovary	53	21-70
0.166	Colon Prostate	85	22-70
-0.174	Colon Testis	38	22-70
0.060	Colon Blood	45	22-70
0.433	Kidney Lung	26	39-68
0.181	Kidney Muscle	12	42-70
0.524	Kidney Ovary	11	42-68
0.351	Kidney Prostate	30	36-70
-0.471	Kidney Testis	27	36-70
0.448	Kidney Blood	24	36-70
0.026	Lung Muscle	25	31-67
-0.111	Lung Ovary	51	22-70
0.167	Lung Prostate	73	22-70
-0.300	Lung Testis	33	25-68
0.378	Lung Blood	37	22-68
0.540	Muscle Ovary	12	34-70
0.340	Muscle Prostate	16	31-70
-0.398	Muscle Testis	11	31-70
0.487	Muscle Blood	11	31-70
0.368	Ovary Blood	9	42-66
-0.234	Prostate Testis	39	22-70
0.308	Prostate Blood	33	22-70
-0.301	Testis Blood	27	22-70

Supplementary Table 11. Linear regression results of aging clocks with leukocytes%, age and the interaction effects.

Supplementary Table 12. Linear regression of age acceleration on smoking, sex, BMI, and telomere length (non-sex specific tissues only).

Observations	<i>Blood</i>		<i>Colon</i>		<i>Kidney</i>		<i>Lung</i>		<i>Muscle</i>	
	51		205		47		194		43	
	<i>Beta</i>	<i>p</i>	<i>Beta</i>	<i>p</i>	<i>Beta</i>	<i>p</i>	<i>Beta</i>	<i>p</i>	<i>Beta</i>	<i>p</i>
Horvath										
Smoking	3.76	0.055	0.63	0.328	-4.13	0.003	-0.39	0.593	-3.34	0.039
Sex	2.43	0.250	0.14	0.820	-1.14	0.368	-0.13	0.857	-1.84	0.219
BMI	0.53	0.009	0.13	0.085	-0.32	0.034	0.17	0.050	0.09	0.581
TQI	1.26	0.738	-0.59	0.421	-4.33	0.009	-0.18	0.901	-0.45	0.825
Hannum										
Smoking	1.03	0.565	-3.43	0.106	-0.40	0.738	1.96	0.005	-1.83	0.152
Sex	1.36	0.488	-1.49	0.470	-0.33	0.775	0.01	0.991	-2.25	0.065
BMI	0.15	0.398	0.14	0.566	-0.07	0.609	0.12	0.138	0.07	0.596
TQI	-3.26	0.357	2.32	0.338	3.02	0.044	-0.54	0.688	-1.94	0.243
EpiTOC										
Smoking	0.00	0.838	-0.01	0.027	-0.00	0.599	0.01	0.003	-0.00	0.883
Sex	0.01	0.288	-0.02	0.015	0.00	0.397	0.00	0.787	-0.00	0.647
BMI	0.00	0.462	0.00	0.372	0.00	0.485	0.00	0.198	-0.00	0.949
TQI	-0.01	0.714	-0.01	0.303	0.00	0.851	-0.01	0.020	-0.00	0.388
PhenoAge										
Smoking	1.62	0.557	-3.53	0.200	-1.92	0.369	4.92	<0.001	-0.97	0.596
Sex	-0.26	0.931	1.05	0.694	-2.42	0.241	2.37	0.024	0.05	0.978
BMI	0.02	0.954	0.11	0.734	-0.05	0.834	-0.10	0.418	0.15	0.452
TQI	-1.26	0.815	5.64	0.074	6.02	0.023	-5.49	0.009	-1.45	0.544
EpiClock										
Smoking	3.82	0.026	-1.52	0.128	-0.98	0.454	2.00	0.001	-1.96	0.104
Sex	2.99	0.106	-1.20	0.215	-0.85	0.498	0.65	0.232	0.44	0.692
BMI	0.30	0.080	0.08	0.501	-0.01	0.967	0.07	0.284	0.14	0.285
TQI	0.54	0.868	0.19	0.869	-0.09	0.957	-1.85	0.095	-0.19	0.900
AltumAge										
Smoking	6.96	0.024	-0.69	0.557	-3.49	0.071	3.64	0.002	-2.22	0.313
Sex	4.15	0.209	1.88	0.099	0.77	0.674	1.40	0.218	0.23	0.911
BMI	0.70	0.024	0.29	0.039	-0.14	0.515	0.16	0.240	0.26	0.280
TQI	-1.05	0.858	-1.52	0.257	-3.76	0.107	-1.96	0.392	2.30	0.422
Zhang										
Smoking	-2.32	0.214	-2.18	0.040	-0.095	0.940	0.180	0.004	-3.82	0.086
Sex	3.12	0.126	0.166	0.871	-0.725	0.555	0.275	0.693	0.150	0.941
BMI	0.007	0.967	0.129	0.303	0.014	0.920	0.098	0.239	0.122	0.596
TQI	-14.3	<0.001	1.83	0.130	-1.62	0.296	-2.13	0.129	-0.202	0.942
Pace										
Smoking	0.009	0.898	0.064	0.014	0.420	0.224	0.083	<0.001	0.006	0.805
Sex	-0.034	0.664	0.002	0.938	-0.105	0.917	-0.029	0.088	0.045	0.039
BMI	-0.003	0.651	-0.001	0.632	0.001	0.722	-0.002	0.226	0.001	0.596
TQI	-0.173	0.222	-0.064	0.030	-0.091	0.032	0.486	0.150	0.038	0.201

The effect of sex is in reference to male and the effect of smoking is reference to non-smokers.

Supplementary Table 13. Linear regression of age acceleration on smoking, BMI, telomere length (sex specific tissues only).

Observations	Breast		Ovary		Prostate		Testis	
	36		142		111		45	
	<i>Beta</i>	<i>p</i>	<i>Beta</i>	<i>p</i>	<i>Beta</i>	<i>p</i>	<i>Beta</i>	<i>p</i>
Horvath								
Smoking	-0.39	0.841	1.29	0.078	-0.81	0.438	4.62	0.032
BMI	0.46	0.049	-0.06	0.511	0.16	0.225	-0.29	0.217
TQI	0.32	0.913	-0.68	0.591	-3.88	0.023	-3.55	0.039
Hannum								
Smoking	-2.28	0.073	-0.65	0.339	-1.39	0.234	1.23	0.279
BMI	0.41	0.008	0.02	0.775	0.26	0.075	-0.26	0.045
TQI	-0.31	0.868	0.97	0.405	-4.58	0.017	-1.88	0.042
EpiTOC								
Smoking	-0.01	0.241	-0.00	0.301	0.00	0.979	0.00	0.204
BMI	-0.00	0.856	-0.00	0.262	-0.00	0.862	0.00	0.546
TQI	0.01	0.431	0.00	0.669	-0.01	0.116	0.00	0.457
PhenoAge								
Smoking	-4.20	0.193	0.69	0.449	-0.38	0.838	1.94	0.205
BMI	0.56	0.139	-0.00	0.996	0.40	0.091	0.12	0.477
TQI	8.09	0.098	0.25	0.872	-4.84	0.110	-0.43	0.727
EpiClock								
Smoking	0.02	0.991	0.02	0.973	0.12	0.933	5.12	0.037
BMI	0.20	0.394	0.01	0.870	0.08	0.644	-0.27	0.327
TQI	3.82	0.213	1.48	0.145	-5.38	0.017	-5.54	0.006
AltumAge								
Smoking	-5.55	0.125	2.02	0.185	-1.27	0.354	6.82	0.103
BMI	0.44	0.296	-0.02	0.909	0.08	0.660	-0.50	0.286
TQI	0.76	0.886	1.04	0.692	-6.53	0.004	-6.38	0.059
Zhang								
Smoking	-1.32	0.339	0.009	0.995	-0.378	0.677	6.45	0.034
BMI	0.297	0.072	-0.194	0.154	0.196	0.088	-0.085	0.799
TQI	1.31	0.542	0.906	0.651	-4.38	0.004	-4.34	0.073
Pace								
Smoking	0.118	0.003	0.007	0.547	0.334	0.222	-0.008	0.588
BMI	0.008	0.082	0.001	0.518	-0.006	0.108	0.004	0.032
TQI	0.082	0.146	-0.009	0.669	-0.075	0.093	0.005	0.700

The effect of smoking is in reference to non-smoking.